Heliyon 10 (2024) e27873

Contents lists available at ScienceDirect

Heliyon

journal homepage: www.cell.com/heliyon

Research article

Comprehensive single-cell analysis reveals heterogeneity of fibroblast subpopulations in ovarian cancer tissue microenvironment

Bo Ding [a,1], Zheng Ye [b,1], Han Yin [a], Xin-Yi Hong [a], Song-wei Feng [a], Jing-Yun Xu [a], Yang Shen [a,*]

[a] Department of Obstetrics and Gynecology, Zhongda Hospital, School of Medicine, Southeast University, Nanjing, China
[b] Institute of Computational Science and Technology, Guangzhou University, Guangzhou, 510006, Guangdong, China

ARTICLE INFO

Keywords:
Ovarian cancer
Cancer associated fibroblasts
Tumor micro-environment
scRNAseq
Mendel randomization

ABSTRACT

Background: Ovarian cancer, as a highly malignant tumor, features the critical involvement of tumor-associated fibroblasts in the ovarian cancer tissue microenvironment. However, due to the apparent heterogeneity within fibroblast subpopulations, the specific functions of these subpopulations in the ovarian cancer tissue microenvironment remain insufficiently elucidated.
Methods: In this study, we integrated single-cell sequencing data from 32 ovarian cancer samples derived from four distinct cohorts and 3226 bulk RNA-seq data from GEO and TCGA-OV cohorts. Utilizing computational frameworks such as Seurat, Monocle 2, Cellchat, and others, we analyzed the characteristics of the ovarian cancer tissue microenvironment, focusing particularly on fibroblast subpopulations and their differentiation trajectories. Employing the CIBERSORTX computational framework, we assessed various cellular components within the ovarian cancer tissue microenvironment and evaluated their associations with ovarian cancer prognosis. Additionally, we conducted Mendelian randomization analysis based on *cis*-eQTL to investigate causal relationships between gene expression and ovarian cancer.
Results: Through integrative analysis, we identified 13 major cell types present in ovarian cancer tissues, including $CD8^+$ T cells, malignant cells, and fibroblasts. Analysis of the tumor microenvironment (TME) cell proportions revealed a significant increase in the proportion of $CD8^+$ T cells and $CD4^+$ T cells in tumor tissues compared to normal tissues, while fibroblasts predominated in normal tissues. Further subgroup analysis of fibroblasts identified seven subgroups, with the MMP11+Fib subgroup showing the highest activity in the TGFβ signaling pathway. Single-cell analysis suggested that oxidative phosphorylation could be a key pathway driving fibroblast differentiation, and the ATRNL1+KCN + Fib subgroup exhibited chromosomal copy number variations. Prognostic analysis using a large sample size indicated that high infiltration of MMP11+ fibroblasts was associated with poor prognosis in ovarian cancer. SMR analysis identified 132 fibroblast differentiation-related genes, which were linked to pathways such as platinum drug resistance.
Conclusions: In the context of ovarian cancer, fibroblasts expressing MMP11 emerge as the primary drivers of the TGF-beta signaling pathway. Their presence correlates with an increased risk

* Corresponding author. Department of Obstetrics and Gynecology, Zhongda Hospital, School of Medicine, Southeast University, Nanjing, 210009, China.
E-mail address: shenyang@seu.edu.cn (Y. Shen).
[1] These authors contributed equally to this work.

https://doi.org/10.1016/j.heliyon.2024.e27873
Received 13 January 2024; Received in revised form 4 March 2024; Accepted 7 March 2024
Available online 17 March 2024

of adverse ovarian prognoses. Additionally, the genetic regulation governing the differentiation of fibroblasts associated with ovarian cancer correlates with the emergence of drug resistance.

1. Introduction

Ovarian cancer, a prevalent gynecologic malignancy, remains a significant challenge in women's health [1–3]. Its highly invasive nature and propensity for metastasis contribute to poor prognosis and limited treatment options [4]. The disease's diverse pathological manifestations, coupled with a dearth of effective screening methods and the absence of clear clinical indicators, result in an alarming 75% of patients only being diagnosed at an advanced stage, casting a pall over prognosis [5]. The cornerstone of ovarian cancer treatment currently lies in surgical cytoreduction to R0, with a chemotherapy cocktail of carboplatin and paclitaxel administered subsequently [6]. Post first-line chemotherapy, maintenance therapies may be introduced, encompassing poly ADP-ribose polymerase (PARP) inhibitors, anti-angiogenesis agents, or monoclonal antibodies [7]. While the initial treatment responsiveness is high, with more than 80% of patients demonstrating sensitivity, a majority subsequently develop resistance to chemotherapy, culminating in advanced recurrence and, ultimately, death [8]. The overall 5-year survival rate for patients in advanced stages hovers at a dismal 30%, with even resource-rich nations such as the United States reporting a slightly improved yet still bleak rate of about 47% [3]. These disheartening statistics underscore the pressing need for a more nuanced understanding of the heterogeneity and biological underpinnings of ovarian cancer. Such knowledge is crucial to develop or refine treatment stratagems and bolster the quality of life for those affected by this malignancy.

Parallel to these advancements, another research sphere has surfaced in the form of the tumour microenvironment (TME), marking an increasingly prominent role in ovarian cancer studies [9]. The ovarian cancer TME presents a sophisticated arrangement of diverse cellular and non-cellular components that collaborate to establish a supportive scaffold for tumour proliferation and metastasis [10]. This complex environment, filled with immune cells, stromal fibroblasts, endothelial cells, and components of the extracellular matrix, functions as a dynamic stage where ongoing interactions with tumor cells take place, greatly influencing the trajectory of disease advancement [11].

Among the TME constituents, cancer-associated fibroblasts (CAFs) have ascended the stage as crucial actors in the biology of ovarian cance [12]. CAFs are a heterogenous assembly of activated fibroblasts that champion tumour growth, angiogenesis, and metastasis, via paracrine signalling and remodelling of the extracellular matrix [13]. Recent studies have shed light on the multifaceted roles of CAFs, emphasising their capacity to modulate immune responses, facilitate tumour cell invasion, and harbour therapeutic resistance [14–16]. Discerning the molecular characteristics and functional heterogeneity of CAFs holds the key to unveiling innovative therapeutic targets and catalysing the development of pioneering treatment strategies. Quiescent or resting Cancer-Associated Fibroblasts (CAFs) are typically characterized by their expression of Vimentin (VIM) [17]. These quiescent CAFs principally represent normal fibroblasts and generally exhibit lower proliferative and metabolic capabilities compared to their activated counterparts [12]. Activated CAFs, on the other hand, demonstrate a diverse array of markers, which include α-smooth muscle actin (α-SMA), fibroblast activation protein (FAP), low caveolin1 (CAV1), CD10, integrin β1 (CD29),and G protein-coupled receptor 77 (GPR77) [18]. The transformation of resting CAFs into the active state can be initiated via several pathways. These include the Janus kinase/Signal Transducer and Activator of Transcription (JAK/STAT) signaling pathway, the focal adhesion kinase (FAK) pathway [19], the Hedgehog signaling pathway [20], and the platelet-derived growth factor signaling (PDGF) pathway [21].Several cytokines, encompassing interleukins IL-1 and IL-6, nuclear factor kappa-light-chain-enhancer of activated B cells (NF-κB), and Transforming Growth Factor-beta (TGF-β), are also recognized as playing crucial roles in the CAF activation process [2]. Despite the significant progress made in ovarian cancer research, several challenges and gaps remain. Limited access to well-annotated clinical specimens, heterogeneity within tumor samples, and the lack of standardized research methodologies hinder comprehensive investigations into the disease. Furthermore, the precise mechanisms by which CAFs interact with tumor cells and other components of the TME require further elucidation. Moreover, there remains a paucity of comprehensive research on the differentiation mechanisms of these ovarian cancer-associated fibroblasts. Additionally, the heterogeneity of CAFs within tumor tissues is further evidenced by their distinct subtypes, the roles of which in the tumor microenvironment necessitate further investigation.

This study aims to address these knowledge gaps and achieve a comprehensive understanding of ovarian cancer and its intricate tumor microenvironment (TME), with a particular emphasis on the pivotal role of cancer-associated fibroblasts (CAFs). By harnessing integrated datasets from multiple single-cell sequencing experiments and leveraging extensive patient cohorts, our objective is to unveil the intricate molecular mechanisms that regulate the interplay between CAFs and the tumor microenvironment. Additionally, we are committed to exploring the regulatory patterns and heterogeneity of fibroblast differentiation, along with utilizing the drug-targeting Mendelian randomization approach to explore potential therapeutic avenues for ovarian cancer. Through confronting the current challenges and advancing our comprehension of ovarian cancer biology, our endeavors aspire to bring forth substantial improvements in patient care, ultimately enhancing the prognosis of those afflicted by this formidable ailment.

1.1. Data Source

In this comprehensive investigation, we harnessed a diverse array of datasets, encompassing both single-cell sequencing and bulk RNA sequencing data, to delve into the intricate molecular attributes and underlying mechanisms of ovarian cancer. Our repertoire of single-cell sequencing datasets comprised EMTAB8107 [22], GSE151214 [23], GSE154600 [24], and GSE184880 [25]. Among these,

EMTAB8107 encompassed a collection of 7 samples, including 5 ovarian cancer specimens and 2 normal controls. Meanwhile, GSE151214 encompassed 8 ovarian cancer samples, and GSE154600 encompassed 5. The GSE184880 dataset consisted of 12 ovarian cancer samples and 5 matched normal control samples (**Data Source1**).

Furthermore, our investigative efforts extended to bulk RNA sequencing data, encompassing specimens from the TCGA OV [26] initiative, in addition to data curated from platforms: GPL96, GPL570, GPL2986, GPL6480, and GPL7759. This assemblage of bulk RNA sequencing datasets was representative of 3226 samples, endowing us with an extensive gene expression landscape. For RNA-seq data, we standardized the data using the 'voom' function from the limma package. For data sourced from chip arrays, we utilized logp1 normalization. To address batch effects within datasets from the same platform, we applied the 'combat' function from the sva package [27]. This comprehensive approach ensures robust normalization and batch effect removal, facilitating accurate downstream analysis and interpretation. The integrated analysis of these datasets was instrumental in providing a panoramic view of global gene expression alterations and underlying biological processes in ovarian cancer (Data Source2).

Beyond the aforementioned datasets, we harnessed the power of Genome-Wide Association Studies (GWAS) through the ieu-b-4963 ovarian cancer cohort data (https://gwas.mrcieu.ac.uk/about) [28]. This repository encompasses an expansive collection of ovarian cancer patient samples, offering a fertile ground for probing genetic variations and susceptibility genes linked to ovarian cancer. Moreover, we harnessed *cis*-eQTL (*cis*-expression quantitative trait loci) data from the GTEx V8 database [29], specifically focusing on tissue samples pertinent to the ovary. This facet of the analysis aimed to unravel the intricate genetic regulatory networks and factors underpinning ovarian cancer.

Through the judicious integration of these heterogeneous datasets, we achieved a panoramic and precise portrayal of the ovarian cancer molecular landscape. This integrative approach enabled the identification of pivotal biological features and latent therapeutic targets. The holistic analysis of this data confluence serves as the bedrock for our study, augmenting our understanding of ovarian cancer progression and providing crucial insights into therapeutic avenues.

1.2. Single-cell data preprocessing

In the scope of this study, we employed the SCTransformer module within Seurat.v4.1 [30] to undertake the standardization of single-cell sequencing data. SCTransformer represents a widely used technique adept at mitigating the influence of sequencing batch effects. This instrumental process enables robust comparisons and integrated analyses across diverse datasets and experimental batches. By subjecting the data to standardization, we effectively mitigate batch effects stemming from experimental conditions and technical disparities, thereby ensuring data consistency and reliability. Employing the RunPCA algorithm, we executed linear dimensionality reduction on the amalgamated single-cell sequencing data. The first 30 principal components were selected to facilitate subsequent non-linear dimensionality reduction and cluster analysis.

Moreover, the integration of single-cell data was accomplished through the utilization of the Harmony [31] algorithm. Harmony, grounded in batch adjustment principles, proficiently eliminates batch effects across distinct data cohorts. This strategic employment of the Harmony algorithm facilitated the integration of samples from disparate datasets, thereby yielding a more comprehensive and harmonized single-cell dataset. This integration strategy markedly reduces technical biases, consequently enhancing the precision of subsequent cell type identification and analytical endeavors.

The cell type annotation of single-cell data was performed employing the SingleR [32]. SingleR hinges upon reference gene expression profiles, facilitating the comparison and annotation of individual cell gene expression patterns against a reference database of cell types. Utilizing PTPRC as a marker for immune cells, EPCAM for epithelial/malignant cells, and PECAM1/CD31 for stromal cells, we further annotated cell types using the CellMetainfo from the E-MTAB-8107 dataset in the TISCH2 [33] database. Our analysis revealed 2211 B cells, 16,323 CD4 T cells, 33,616 CD8 T cells, 44,810 fibroblast cells, 5483 endothelial cells, 5900 epithelial cells, 12,752 M1 macrophages, 26,293 malignant cells, 906 mast cells, 9163 monocytes, 5828 myofibroblasts, 14,148 NK cells, and 3834 plasma cells. Subsequent subtype analysis of fibroblast and malignant cells identified 7 and 3 subtypes, respectively. Leveraging the FindAllMarkers function, we identified differentially expressed genes for each cell type using a one vs. others strategy, and assigned names to these clustered cells based on marker genes. This comprehensive analysis sheds light on the intricate cellular landscape of the studied tissue.

The amalgamation of Seurat's SCTransformer, Harmony, and SingleR methodologies begets a robust and accurate analytical framework for the analysis of single-cell sequencing data. Such an analytical arsenal serves to elucidate and juxtapose cell types and states amongst various samples, unveiling the cellular heterogeneity and dynamic changes pivotal to ovarian cancer progression. Ultimately, this analytical paradigm contributes vital cues for an in-depth comprehension of the molecular mechanisms underpinning ovarian cancer and its disease trajectory.

1.3. Fibroblast differentiation assessment

In this study, we harnessed advanced tools, including Cytotrace [34] and Monocle2 [35], to illuminate the intricate process of fibroblast differentiation within the context of ovarian cancer. Cytotrace, a sophisticated single-cell transcriptome analysis tool, emerged as our cornerstone for deciphering and tracking the subtle cellular shifts occurring during development and differentiation. With Cytotrace's capabilities, we adeptly traced the metamorphic trajectory of fibroblasts within ovarian cancer tissues, thereby elucidating their dynamic adaptations throughout the course of tumor evolution.

Monocle2, an acclaimed analytical apparatus tailored to single-cell RNA sequencing data, emerged as another invaluable asset in our arsenal. Particularly designed to delve into cell differentiation and developmental processes, Monocle2 uncovered key

transcriptional players and pivotal shifts in gene expression profiles intrinsic to fibroblast differentiation. This revelation served as a gateway to unmasking the inherent functionality and distinctive attributes of these fibroblasts.

Synthesizing the insights harvested from Cytotrace and Monocle2, a comprehensive vista of fibroblast differentiation in the ovarian cancer milieu emerged. The combined prowess of these analytical tools unveiled a systematic voyage through fibroblast differentiation, chronicling their metamorphosis from a primitive undifferentiated state to a refined, specialized one. This voyage into the labyrinth of fibroblast differentiation unlocked a profound comprehension of their roles and contributions within the tapestry of ovarian cancer progression.

Incorporating the transformative power of these analytical instruments enabled us to plumb the depths of fibroblast differentiation nuances in the realm of ovarian cancer. This, in turn, furnished us with the potent insights required to unravel their pivotal roles in orchestrating ovarian cancer's evolutionary dance. This endeavor assumes profound significance in the context of our comprehensive understanding of the ovarian tumor microenvironment, shedding light on the intricate symphony between malignant cells and fibroblasts. As our knowledge matures, it also offers navigational guidance for pioneering novel therapeutic paradigms and refining prognostic avenues for patients.

1.4. Deciphering the Co-expression landscape of fibroblasts

Within our study, we harnessed the Weighted Gene Co-expression Network Analysis (WGCNA) [36,37] methodology to meticulously unravel the intricate fabric of regulatory networks governing fibroblast behavior. WGCNA, a well-regarded analytical tool in the gene expression realm, emerged as the linchpin in decoding and exposing the underpinnings of co-expression patterns among genes. These insights paved the way for the meticulous construction of co-expression networks grounded in these patterns.

Preliminarily, genes with a presence in a minimum of 5% of cells underwent judicious screening. Subsequent to this screening, cells exhibiting akin expression profiles (with a minimum of 10 cells) were amalgamated into what we term "MetaCells." Our investigative lens then focused on these amalgamated MetaCells, steering them through the WGCNA analysis.

Through the prism of WGCNA, genes showcasing intimately interwoven expression patterns within fibroblasts were adroitly apportioned into distinct modules. This modular unraveling, akin to uncovering clusters of interconnected genes, not only laid bare gene sets intrinsically linked to fibroblast differentiation and function, but also cast light on the intricate regulatory interplay threading through different modules.

By delving into the labyrinthine co-expression regulatory network residing within fibroblasts, we cast a luminous glow on the pivotal regulatory pathways and master regulators steering the course of ovarian cancer-associated fibroblasts. This network-centric analysis method, akin to a navigator's compass, guided us in identifying the latent target genes and intricacies of regulatory mechanisms, thereby unmasking the multifaceted functional tapestry and roles that fibroblasts assume within the context of ovarian cancer.

1.5. Analysis of tumor cell copy number variations

In our investigation, we harnessed the InferCNV [38] method to delve into the copy number variations (CNVs) within tumor cells. InferCNV, grounded in single-cell RNA sequencing data, serves as an analytical tool for deciphering alterations in gene copy numbers within cells.

By employing InferCNV, we derived copy number information from single-cell RNA sequencing data, thereby discerning amplifications or deletions in chromosomal segments present within tumor cells. This methodology aids in uncovering copy number variation events intrinsic to tumor cells, thereby revealing pivotal genes and pathways entwined with tumor development and progression.

The copy number variations inherent within tumor cells play a pivotal role in tumor development and progression. They have the capacity to influence the expression levels of critical tumor suppressor genes and oncogenes, thereby impacting tumor cell proliferation, metastasis, and treatment resistance. Through the analysis of copy number variations within tumor cells, we can identify potential oncogenes and tumor suppressor genes, thus shedding light on genetic variations and adaptive evolutionary processes within tumor cells.

The copy number variation (CNV) score in the integrated scRNAseq data with fibroblast cells was calculated based on the single-cell transcriptomic profiles using InferCNV (https://github.com/broadinstitute/inferCNV (version 1.10.1)) (accessed on August 20, 2021). Stromal cells including immune cells and endothelial cells were selected as references. For the inferCNV analysis, the following parameters were used: "denoise," default hidden markov model settings, and a value of 0.1 as the "cutoff" value. Finally, the subclusters with relatively higher CNV scores were considered malignant cells.

1.6. Transcription factor activity analysis

In our investigation, we harnessed the potential of dorothea [39] tools to dissect transcription factors within single-cell transcriptomic data. Dorothea serves as a transcription factor-centric gene expression regulatory network instrument, aiming to infer transcription factor activity across diverse cellular types and states. By harnessing transcription factor binding site data and DNA co-localization modification information, Dorothea constructs a model of transcription factor activity. Encompassing nearly 2000 distinct human and mouse tissue and cell type-specific transcription factors and regulatory elements, Dorothea empowers the analysis of transcription factor activity within single-cell transcriptomic data, thereby revealing their latent roles in cellular type and state regulation.

By applying tools such as Dorothea, we unearth critical transcription factors from single-cell transcriptomic data, thereby deducing their activity across a spectrum of cell types and states. This transcription factor enrichment analysis furnishes insights into the role of transcriptional regulatory networks within ovarian cancer development, unveiling the biological functions and latent regulatory mechanisms of transcription factors. Moreover, by amalgamating with other functional enrichment analysis methodologies such as gene pathway enrichment analysis and transcription factor-target gene regulatory network analysis, we can delve even deeper into the pivotal role of transcription factors in ovarian cancer, thereby affording critical insights for the development of novel therapeutic strategies and prognostication of patient outcomes.

1.7. Bulk-RNAseq deconvolution analysis

In our study, we employed the CIBERSORTx [40] tool for deconvolution analysis of bulk-RNAseq data. CIBERSORTx is a widely used tool in the field of bioinformatics, designed to infer the relative proportions of different cell types from mixed cell samples' gene expression data.

By utilizing CIBERSORTx, we were able to deconvolve the complex mixture of cell populations within Bulk-RNAseq data into individual cell types and calculate their relative abundances within the samples. This deconvolution analysis method facilitated a quantitative assessment of the presence of distinct cell types, enabling further exploration of their functions and interactions in the context of ovarian cancer.

CIBERSORTx leverages machine learning algorithms and predefined reference gene expression profiles to perform deconvolution calculations on bulk-RNAseq data. It accomplishes this by comparing the gene expression profiles of samples to reference profiles, thereby inferring the relative proportions of different cell types. This approach, based on known gene expression patterns and pattern recognition techniques, achieves highly accurate deconvolution of cell composition within Bulk-RNAseq data.

To begin our analysis, we selected 100 cells from each of the 21 cell types within the merged scRNAseq data, creating an expression profile matrix. Subsequently, we constructed a signature matrix using the "Create Signature Matrix" module of CIBERSORTx (kappa = 999, q-value = 0.01, No.Barcode Genes = 300–500). Next, we conducted deconvolution of the bulk RNAseq data using the "Impute Cell Fractions" module. We implemented the S-mode to mitigate batch effects between single-cell and bulk RNAseq data, setting permutations to 500. Ultimately, this process yielded absolute scores for the 21 cell types present in the bulk RNAseq data from six sources. Through deconvolution analysis, we obtained valuable information about the various cell types within ovarian cancer samples, including immune cells, fibroblasts, and tumor cells. This quantitative analysis of cell types contributes to a deeper understanding of the tumor microenvironment and cellular composition in ovarian cancer, revealing the interplay between changes in relative cell proportions and the progression of the disease.

1.8. Cell-cell communication analysis

We employed the CellChat [41] algorithm (https://github.com/sqjin/CellChat, version 1.6.1) to elucidate cell-cell interactions [22]. In accordance with the official workflow, we imported the normalized count data from Seurat into CellChat for further processing. The built-in ligand-receptor database in CellChat was utilized to infer intercellular communication. Subsequently, the CellChat algorithm was executed to compute probable interactions and pathways using the "computeCommunProb" and "computeCommunProbPathway" functions. To enhance the robustness of our analysis, we filtered out interactions involving fewer than 10 cells per cell type using the "filterCommunication" function.

1.9. SMR analysis

We implemented an eQTL-based Summary Mendelian Randomization (SMR) analysis, with *cis*-eQTL serving as the instrumental variable (IV), gene expression as the exposure, and ovarian cancer as the outcome, as per the method delineated in the SMR software. As detailed in prior literature [42], SMR employs the tenets of MR to analyze GWAS and eQTL summary statistics concurrently, thereby testing for a pleiotropic association between gene expression and a trait, attributable to a shared, potentially causal variant at a locus. The most significant *cis*-eQTL was utilized in SMR to estimate the gene expression impact on the outcome. The integrity of the genetic variants as IVs is crucial for SMR to yield consistent estimates, necessitating the fulfillment of three assumptions: 1) association with the risk factor (gene expression); 2) absence of association with any confounder of the risk factor-outcome relationship; 3) conditional independence from the outcome given the risk factor and confounders. A P-value less than $1x10^{-5}$ in a linear regression eQTL analysis for each variant indicates a negligible weak instrument bias. In the SMR analysis, we adopted a default threshold of P eQTL = $5x10^{-8}$to select the top associated *cis*-eQTL (within a default window size of 1000 Kb) for the SMR analysis, mitigating the risk of a weak IV. By default, we eliminated SNPs with allele frequency differences >0.2 between any pairwise datasets, including the LD reference sample data, the eQTL summary data, and the GWAS summary data. We also undertook a heterogeneity in dependent instruments (HEIDI) [43] test to assess the presence of linkage in the observed association. The null hypothesis rejection (i.e., PHEIDI <0.05) implies that the observed association might be attributable to two distinct genetic variants in high linkage disequilibrium. In the HEIDI test, we adhered to default settings: removing SNPs in very strong linkage disequilibrium [LD, r2 > 0.9] with the top associated eQTL, and SNPs in low LD or not in LD [r2 < 0.05] with the top associated eQTL; PeQTL<$1.5x10^{-3}$; number of *cis*-SNPs>3 for a HEIDI as HEIDI test loses power if *cis*-SNPs< 3; and maximum eQTLs in a HEIDI test = 20. Multiple testing was adjusted for using the false discovery rate (FDR).

Subsequently, we conducted *cis*-eQTL and SMR analyses for genes related to 21 cell types and Fibroblast differentiation. For each

cell type, eQTLs with a causal relationship with ovarian cancer were examined for gene-drug interaction relationships using The Drug Gene Interaction Database (https://www.dgidb.org).

1.10. Statistical analysis

Statistical analysis and bioinformatical processing were carried out in R version 4.1.0 (https://www.r-project.org/), PLINK 1.9 (https://www.cog-genomics.org/plink/1.9/), and the SMR tool (https://cnsgenomics.com/software/smr/). Rstudio was chosen as the primary working environment, and R packages such as ggplot2, ggpubr, and dittoSeq [44]]were used for the creation of statistical graphs. For the differential expression analysis of single-cell sequencing data, the Wilcoxon test was utilized. Statistically, results with a P-value less than 0.05 were considered significant.

2. Results

2.1. Comparative analysis of tumor microenvironment characteristics in ovarian cancer and adjacent normal tissue

By integrating 32 single-cell sequencing samples across four cohorts (Fig. 1A and B), we identified three primary cell types, namely

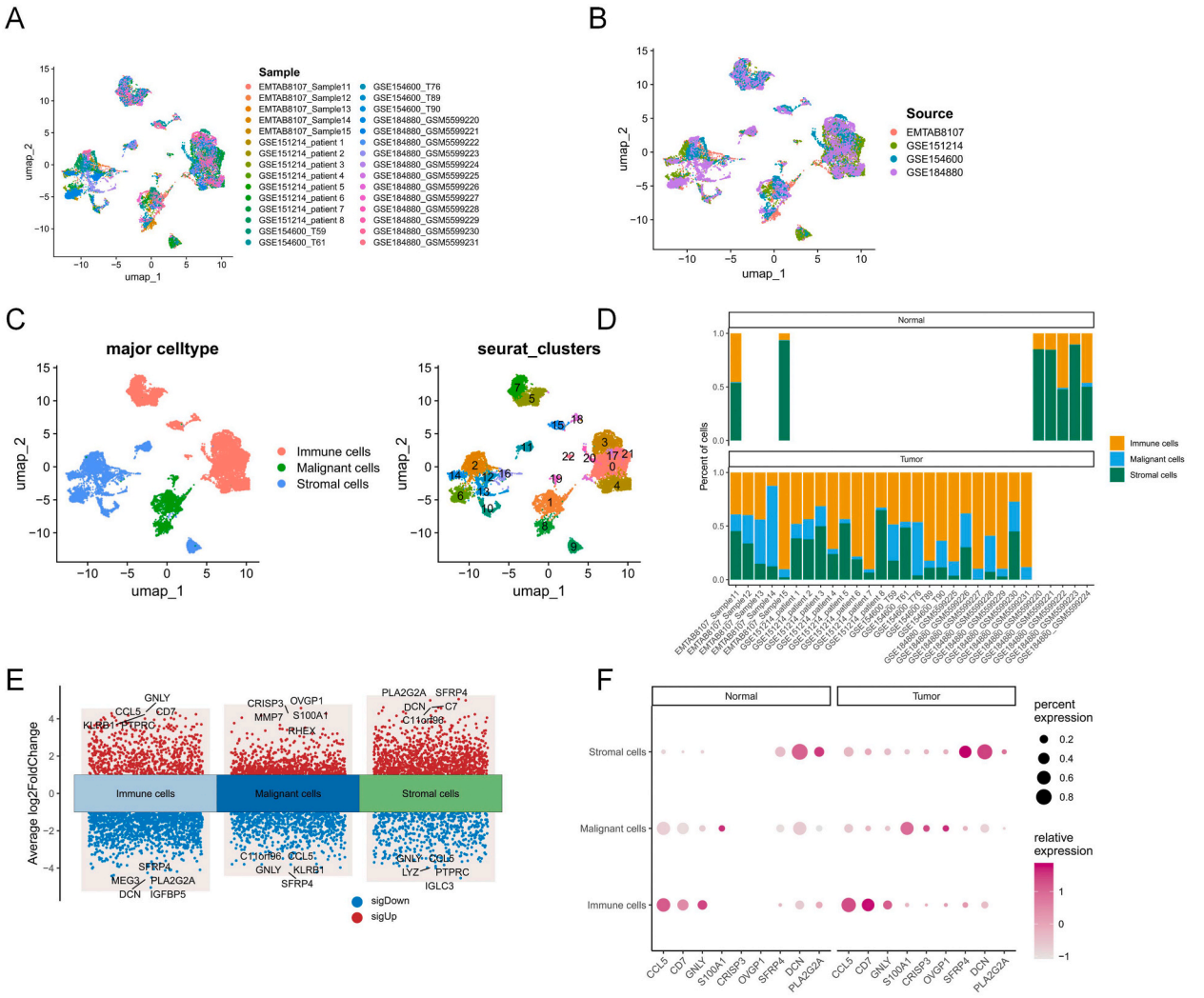

Fig. 1. Integration of single-cell sequencing data. (A, B) Integration of 32 single-cell samples from four cohorts. (C) Major cluster classification reveals three main cell groups: Immune cells, Malignant cells, and Stromal cells. Unsupervised clustering using the Louvain algorithm identifies 23 cell subpopulations. (D) Proportions of the three major cell groups in each single-cell sample. (E) Differentially expressed genes in the three major cell groups (one vs. others, Wilcoxon test, $|\log2FC| > 1$, Adjusted $P < 0.05$). (F) Molecular markers of the three major cell subpopulations in normal tissue and tumor tissue. Due to the minimal proportion of Malignant cells in normal tissue, the expression levels of tumor-related molecular markers are extremely low.

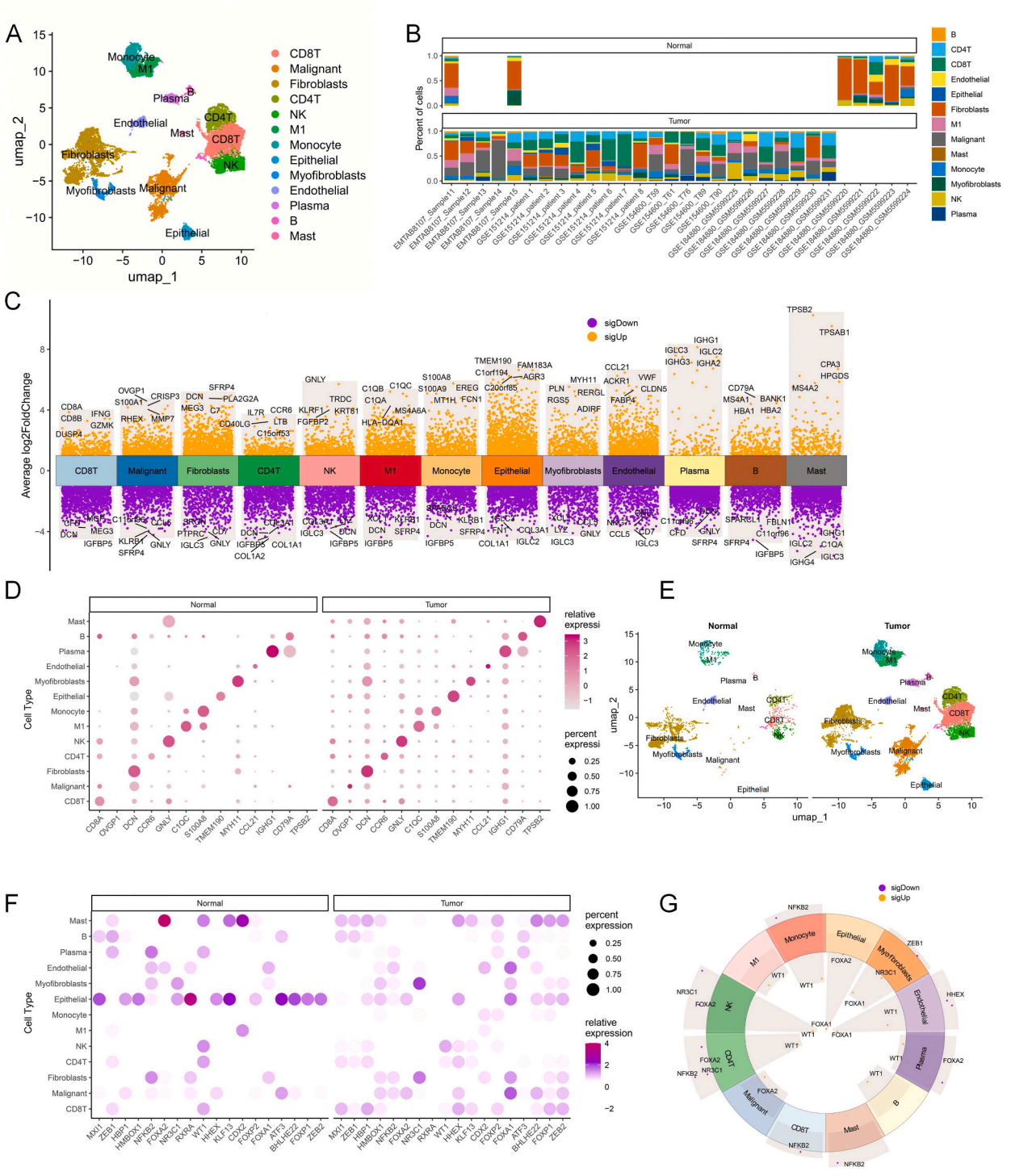

Fig. 2. Annotation of cell subpopulations. (A) The tumor microenvironment of ovarian cancer primarily consists of 13 cell subpopulations. (B) Distribution of the 13 cell subpopulations across the 32 single-cell sequencing samples. (C) Differentially expressed genes in the 13 subpopulations (one vs. others, Wilcoxon Test). (D) Comparison of cell type markers' expression between tumor tissue and normal tissue. (E) Comparison of single-cell subpopulations between tumor tissue and normal tissue. (F) Comparison of differential transcription factor activity between tumor tissue and normal tissue. (G) Comparison of transcription factor activity differences in the 13 cell subpopulations (one vs. others, Wilcoxon Test).

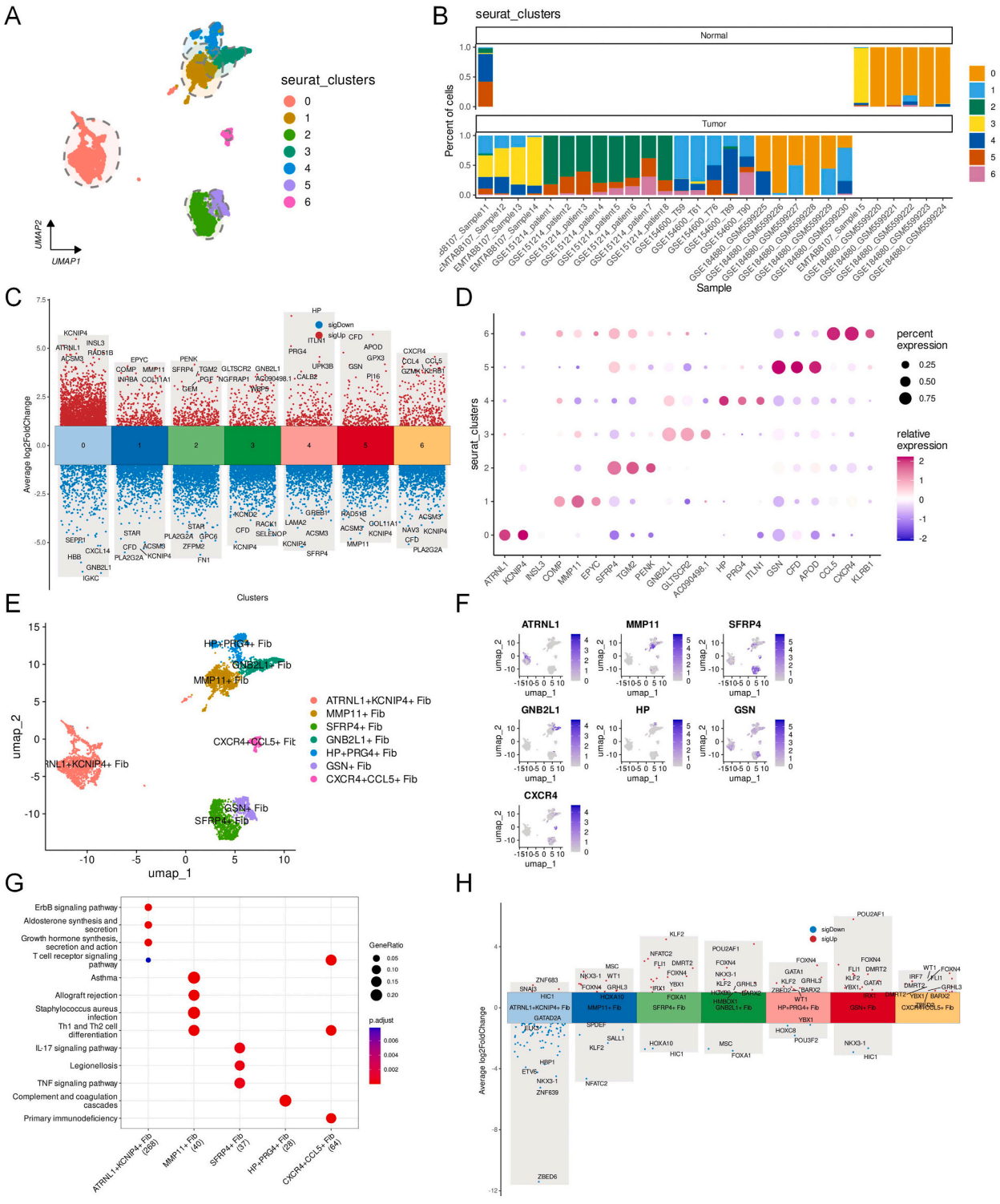

Fig. 3. Analysis of fibroblast subpopulations. (A) Fibroblasts in ovarian cancer are primarily divided into seven subpopulations. (B) Distribution of the seven fibroblast subpopulations in the single-cell sequencing samples. (C) Differentially expressed genes in the seven fibroblast subpopulations (one vs. others, Wilcoxon Test). (D) Molecular markers of the fibroblast subpopulations. (E) Naming of fibroblast subpopulations based on molecular markers. (F) Mapping of major molecular markers of fibroblast subpopulations in the fibroblast subpopulation UMAP dimensionality reduction plot. (G) Functional enrichment analysis results (P.adjust <0.05) of highly expressed genes in fibroblast subpopulations. (H) Differential transcription factor activity in fibroblast subpopulations.

Immune cells, Malignant cells, and Stromal cells (Fig. 1A). We observed that the normal tissue was predominantly composed of Stromal cells, with lesser proportions of Immune cells and Malignant cells (Fig. 1C). Differential expression analysis revealed that the genes highly expressed in Immune cells mainly included GNLY, CCL5, CD7, KLRB1, and PTPRC. In Malignant cells, the highly expressed genes were primarily CRISP3, OVGP1, MMP7, S100A1, and RHEX. Conversely, Stromal cells displayed high expression of genes such as PLA2G2A, SFRR4, DCN, C7, and C11orf96 (Fig. 1D, E, F).

We further subdivided these three primary cell types and identified 23 single-cell subgroups (Fig. S1). Upon annotating these cell subgroups, we discovered 13 major cell clusters, including CD8T, Malignant, Fibroblasts, CD4T, NK, M1, Monocyte, Epithelial, Myofibroblast, Endothelial, Plasma, B, and Mast cells (Fig. 2A).

The tumor microenvironment of ovarian cancer tissue and adjacent normal tissue exhibit significant differences. Normal tissues have a higher proportion of stromal cells, with Fibroblasts being the most numerous within this category. Fibroblasts are more prevalent in normal tissues, while CD8+T and CD4+T cells are more common in tumor tissues (Fig. 2B). To compare the molecular markers of tumor tissues and adjacent normal tissues, we first performed differential expression analysis on all single-cell sequencing data to identify molecular markers for each cell type. We discovered high expression of CD8A, CD8B, IFNG, GZMK, and DUSP4 in CD8+T cells. Malignant cells showed high expression of OVGP1, CRISP3, S100A1, RHEX, and MMP7. Fibroblasts displayed high levels of SFRP4, DCN, PLA2G2A, MEG3, and C7. CD4+T cells were characterized by high expression of IL7R, CCR6, CD40LG, LTB, and C15orf53. NK cells revealed high expression of GNLY, KLRF1, FGFBP2, TRDC, and KRT81. M1 cells showed high expression of C1QA, C1QB, C1QC, MS4A6A, and HLA-DQA1. Monocytes displayed high levels of S100A8, S100A9, MT1H, FCN1, and EREG. Epithelial cells had high expression of TMEM190, C1orf194, AGR3, FAM183A, and C20orf85. Myofibroblasts showed high levels of MYH11, PLN, RGS5, RERGL, and ADIRF. Endothelial cells had high expression of CCL21, VWF, CLDN5, FABP4, and ACKR1. Plasma cells showed high levels of IGLC3, IGHG3, IGHG1, IGLC2, and IGHA2. B cells revealed high expression of CD79A, MS4A1, BANK1, HBA1, and HBA2. Mast cells exhibited high levels of TPSB2, TPSAB1, CPA3, HPGDS, and MS4A2 (Fig. 2C). These genes can serve as molecular markers for these cell types. We compared the top molecular markers in tumor tissues and normal tissues (Fig. 2D and E). We found that OVGP1, a molecular marker for malignant cells, is not expressed in normal cells. Additionally, TPSB2, a molecular marker for Mast cells, is scarcely expressed in normal tissues. This indicates different states of Mast cells in normal and tumor tissues.

Next, we compared transcription factor activity across the 13 cell types (Fig. 2F and G). We found that the transcription factor ZEB1 was downregulated in Myofibroblasts, HHEX in Endothelial cells, FOXA2 in Plasma cells, and NFKB2 in Mast, Monocyte, and CD8T cells. CD4+T cells showed downregulation of FOXA2, NFKB2, and NR3C1. NK cells showed downregulation of FOXA2 and NR3C1. Furthermore, we found that WT1 was significantly upregulated in most cell types, while FOXA1 was significantly upregulated in Epithelial, Myofibroblast, and Endothelial cells.

Finally, we compared the signaling pathway activity levels across the 13 cell types (Fig. S2). We found that Monocyte cells had high NFkB and TNFa activity, regardless of whether they were in normal or tumor tissues. The TGFb signaling pathway activity in Fibroblast cells was notably higher in tumor tissues than in normal tissues, whereas there was no significant difference in Myofibroblasts. Additionally, we noted that Androgen pathway activity in Plasma and Mast cells in normal tissues was significantly higher than in tumor tissues. Lastly, we found that the p53 signaling pathway in Epithelial cells was significantly activated in tumor tissues compared to normal tissues. These findings highlight the distinct transcription factor and signaling pathway activities between the same cell types in tumor and normal tissues.

In summary, Integrating data from 32 single-cell sequencing samples across four cohorts, our study identifies three primary cell types in ovarian cancer: Immune cells, Malignant cells, and Stromal cells. Normal tissue is predominantly composed of Stromal cells, with differential expression analysis revealing distinct molecular markers for each cell type. Subsequent subdivision of these primary cell types unveils 13 major cell clusters, each characterized by specific gene expression profiles. Notably, differences in cell composition and molecular signatures between tumor and normal tissues underscore the complex tumor microenvironment. Moreover, analysis of transcription factor activity and signaling pathway levels reveals dynamic regulatory mechanisms within different cell types, highlighting potential targets for therapeutic intervention. Overall, our findings provide valuable insights into the cellular and molecular landscape of ovarian cancer, shedding light on potential biomarkers and therapeutic targets for further investigation.

2.2. *Subpopulation analysis of fibroblasts*

Cancer-associated fibroblasts (CAFs) significantly influence the prognosis of ovarian cancer [45–47]. Consequently, we focused our investigation on CAFs, identifying seven subgroups of fibroblasts, annotated by their gene markers (Fig. 3A). Notably, cluster0 was primarily present in normal tissues, whereas clusters 1, 2, and 6 were predominantly in tumor tissues (Fig. 3B).

These subtypes are characterized as follows: ATRNL1+KCN + Fib (cluster0, 14,256 cells), MMP11+Fib (cluster1, 8520 cells), SFRP4+Fib (cluster2, 8157 cells), GNB2L1+Fib (cluster3, 4731 cells), HP + PRG4+Fib (cluster4, 3997 cells), GSN + Fib (cluster5, 3308 cells), and CXCR4+CCL5+Fib (cluster6, 1840 cells) (Fig. 3C, D, E, F). This detailed categorization provides insights into the diverse fibroblast populations within the tissue, each potentially contributing distinct roles in the microenvironment.

The ATRNL1+KCNIP4+Fib subtype was characterized by 268 highly expressed marker genes, primarily regulating the ErbB signaling pathway, aldosterone synthesis and secretion, and growth hormone synthesis, secretion, and action. The MMP11+Fib subtype, with 40 high-expression marker genes, was notably enriched in pathways such as asthma, allograft rejection, Staphylococcus aureus infection, and Th1 and Th2 cell differentiation. The SFRP4+ Fib subtype, with 37 marker genes, primarily regulated the IL-17 signaling pathway, legionellosis, and the TNF signaling pathway. The HP + PRG4+Fib subtype, with 28 marker genes, was chiefly enriched in the complement and coagulation cascades signaling pathway. Lastly, the CXCR4+CCL5+Fib subtype, with 64 highly expressed markers, was primarily enriched in the T cell receptor signaling pathway, Th1 and Th2 cell differentiation, and primary

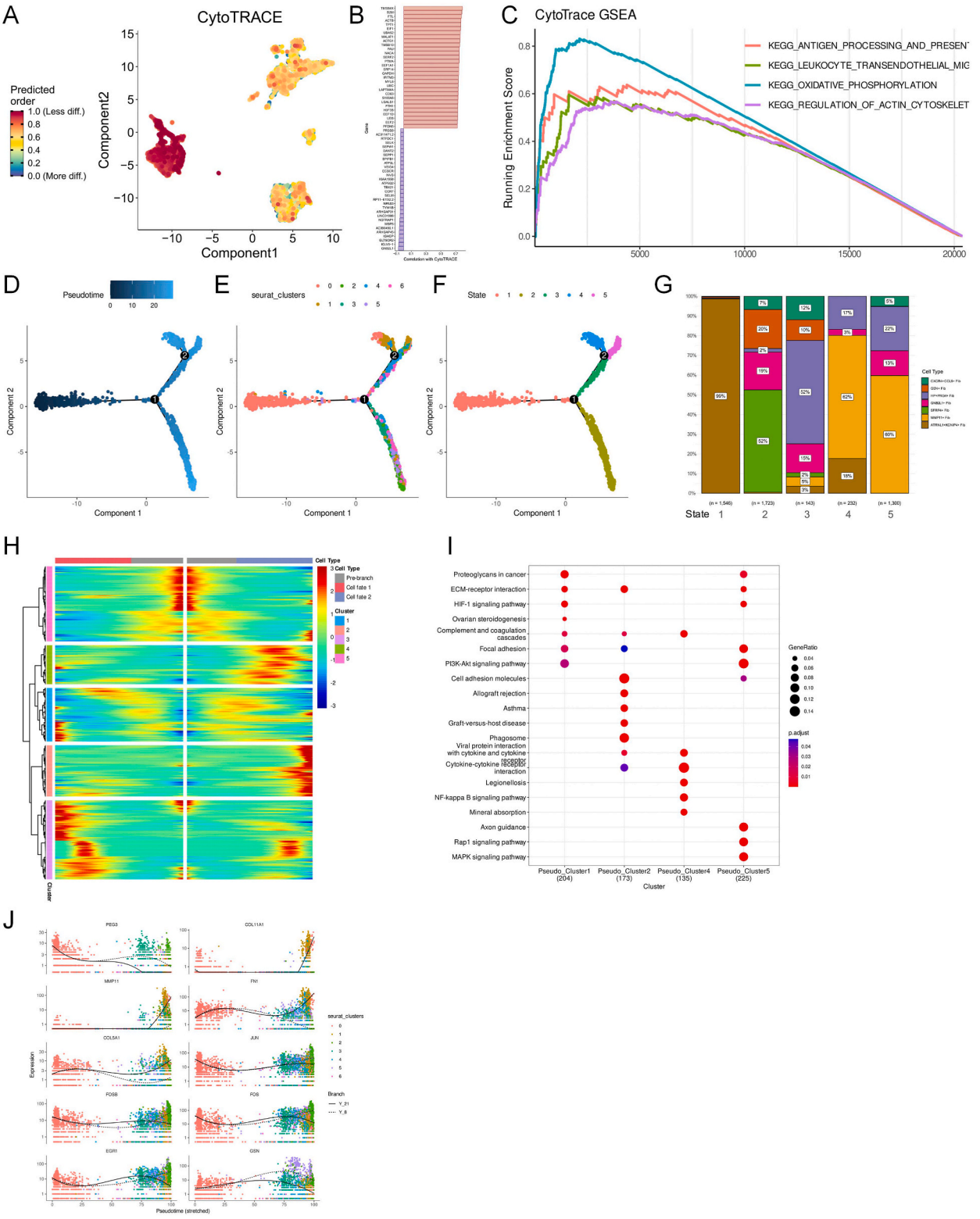

(caption on next page)

Fig. 4. Fibroblast differentiation. (A) Identification of the initial fibroblast subpopulation for differentiation using Cytotrace. (B) Genes associated with fibroblast differentiation identified by Cytotrace. (C) Gene Set Enrichment Analysis (GSEA) for enrichment of pathways related to fibroblast differentiation. A total of 186 pathways from the KEGG database in MSIGDB were analyzed. Gene expression correlation with the differentiation trajectory was used as the ranking statistic. (D) Fibroblast differentiation trajectory obtained using Monocle2. Branch point 1 represents a key point in fibroblast differentiation. (E) Positioning of the seven fibroblast subtypes on the trajectory differentiation plot. (F) Identification of five fibroblast states based on the trajectory differentiation plot (DDRTree dimensionality reduction). (G) Relationship between the five fibroblast states and fibroblast subtypes. State 1 is mainly composed of ATRNL1+KCNIP4+Fib (cluster 0). (H) Fibroblast fate during differentiation. Fibroblasts at branch point 1 have two cell fates. ATRNL1+KCNIP4+Fib differentiates into SFRP4+Fib as Cell fate 1. ATRNL1+KCNIP4+Fib undergoes HP + PRG4+Fib and ultimately differentiates into MMP11+Fib as Cell fate 2. (I) Functional enrichment analysis results for the main modules regulating fibroblast differentiation. (J) Expression levels of genes associated with fibroblast differentiation in relation to pseudotime.

immunodeficiency (Fig. 3G).

In the subsequent transcription factor activity evaluation of the seven fibroblast subgroups (Fig. 3H), we found that transcription factors ZNF683 and SNAI3 were significantly activated in the ATRNL1+KCNIP4+Fib subtype. For the MMP11+ Fib subtype, MSC, WT1, NKX3-1, and FOXN4 were significantly activated. Transcription factors KLF2, NFATC2, FLI1, and DMRT2 showed significant activation within the SFRP4+ Fib subtype. POU2AF1, FOXN4, NKX3-1, and KLF2 were significantly activated in the GNB2L1+Fib subtype. GATA1, FOXN4, and KLF2 were significantly activated in the HP + PRG4+Fib subtype. The GSN + Fib subtype showed significant activation of FOXN4, FLI1, and DMRT2. The CXCR4+CCL5+Fib subtype demonstrated significant activation of WT1, IRF7, and FOXN4. Interestingly, FOXN4 was not activated in the ATRNL1+KCNIP4+Fib subtype, but it was significantly activated in the other fibroblast subtypes, suggesting a possible association between FOXN4 and CAF activation.

Through the screening of transcription factor activity markers, we found that the ATRNL1+KCNIP4+Fib subtype's transcription factor activity markers are ZNF683 and SNAI3. The MMP11+ Fib subtype's transcription factor activity marker is MSC. The SFRP4+Fib subtype's transcription factor activity markers are KLF2 and NFATC2. The GNB2L1+Fib subtype's transcription factor activity marker is NKX3-1. The HP + PRG4+Fib subtype's transcription factor activity marker is GATA1. The GSN + Fib subtype does not have a specific transcription factor activity marker. The CXCR4+CCL5+Fib subtype's transcription factor activity markers are POU2AF1, IRF7, and WT1. In addition, the results of signalling pathway activity analysis by Progeny [48] showed that TGFb signalling pathway activity was the most active in MMP11+Fib(Fig. S3A, B). As the TGFb signalling pathway plays an important role in the remodelling of the tumour microenvironment, cancer development and metastasis [49], this suggests an important role for MMP11+Fib in the tumour microenvironment.

Next, to elucidate the relationships among these fibroblasts, we embarked on an exploration into the cellular differentiation of fibroblasts within ovarian cancer tissue. Harnessing the analytical power of Cytotrace, we discerned that the ATRNL1+KCN + Fib (cluster0) delineates the earliest differentiated fibroblast cohort (Fig. 4A). This intriguing finding posits ATRNL1+KCN + Fib as being primarily dispersed within normal fibroblasts neighboring the cancerous cells, which have not yet embarked on the path of differentiation into cancer-associated fibroblasts. This insight into the initial stages of fibroblast differentiation underlines the dynamic interplay between normal and neoplastic cellular states within the ovarian cancer microenvironment.

We identified the top 20 genes related to cell differentiation (Fig. 4B). Genes such as TMSB4X, B2M, FTL, ACTB, TPT1, and EIF1 exhibit high positive correlations (Pearson corr. >0.7) with the differentiation of fibroblasts. By correlating these genes with the differentiation time obtained from CytoTRACE, we then ranked them. Subsequent GSEA (Gene Set Enrichment Analysis) of these ranked genes (using KEGG gene sets) indicated that KEGG PROTEASOME, KEGG SPLICEOSOME, and KEGG OXIDATIVE PHOSPHORYLATION pathways are significantly associated with the differentiation of fibroblasts (Fig. 4C). Although CytoTRACE can determine the degree of cell differentiation based on gene expression profiles, it cannot provide a precise depiction of the details during cell differentiation. An integrated analysis of fibroblasts revealed seven subgroups. To further disclose the differentiation characteristics of these subgroups, we investigated the gene expression features of these cell subgroups during pseudo-temporal differentiation using Monocle2.

Through Monocle2, we identified the first branching point in Fibroblast differentiation (Fig. 4D, E, F, G). Fibroblasts primarily differentiate towards two directions (Cell fate1, Cell fate2), transitioning from ATRNL1+KCNIP4+Fib (State1) to SFRP4+Fib (State2), that is, Cell fate1. The other differentiation pathway goes through HP + PRG4+Fib(state3) and eventually differentiates into MMP11+Fib (State4,5), that is, Cell fate2 (Fig. 4H). These two differentiation routes underscore the heterogeneity of fibroblast differentiation within tumor tissues, which may be associated with the tumor microenvironment where the fibroblasts reside.

By clustering the genes that regulate cell differentiation, we identified five gene regulatory modules. For example, Pseudo_Cluster1, with minimal fluctuation during fibroblast differentiation, mainly participates in Ovarian steroidogenesis, HIF-1 signaling pathway, PI3K-Akt signaling pathway (Fig. 4I). We selected 10 genes each to represent the gene expression regulation status of these five regulatory modules (Fig. 4J).

To unearth the key regulatory factors governing fibroblast differentiation, we employed Weighted Gene Co-expression Network Analysis (WGCNA) to discern the principal co-expression regulatory modules within the fibroblast population. To ensure the gene expression regulatory network conformed to the scale-free distribution characteristics, a soft threshold of 4 was chosen (Fig. 5A). We identified five co-expression modules (blue, turquoise, green, yellow, brown, red), among which the turquoise module showed a significant negative correlation with other modules (Fig. 5B and C). We selected hub genes from each module for functional enrichment and module scoring (GSVA [50]) (Fig. 5D). Functional enrichment analyses revealed that the blue module (16 hub genes) was primarily involved in transcriptional misregulation in cancer, TNF signaling pathway, and Hepatitis C signaling pathway. The green module (13 hub genes) was largely enriched in antigen processing and presentation, allograft rejection, and graft-versus-host

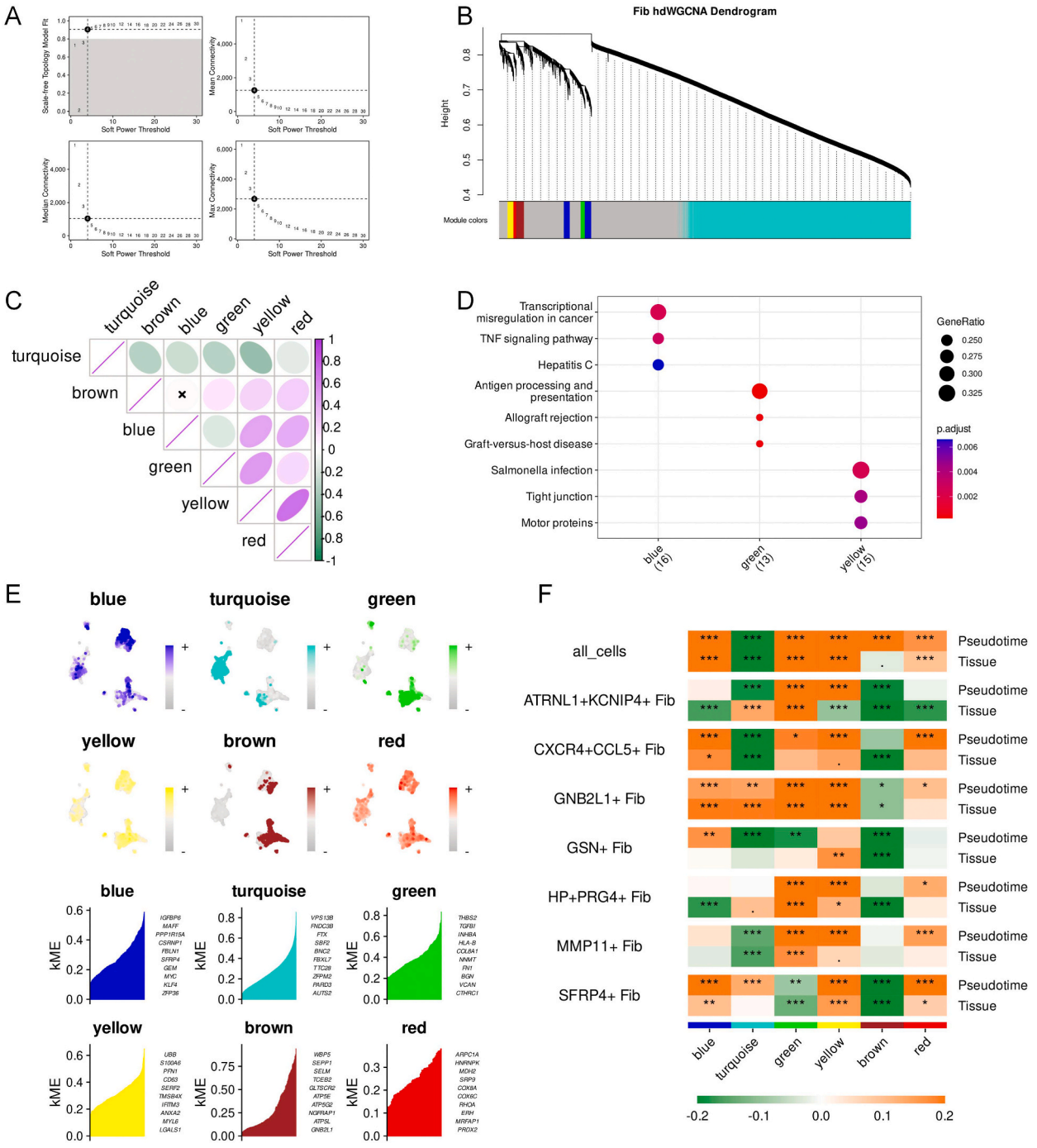

Fig. 5. Co-expression analysis of fibroblast subtypes. (A) Selection of an appropriate soft threshold to ensure that the regulatory network follows a scale-free distribution assumption. (B) Through hdWGCNA, six co-expression regulatory modules were identified in fibroblast subtypes. (C) Correlation between the regulatory modules. Turquoise module shows significant negative correlation with other regulatory modules (brown, blue, green, yellow) (Pearson, $P < 0.05$). (D) Functional enrichment analysis of the regulatory modules. (E) Mapping of GSVA scores of hub genes in the regulatory modules onto the UMAP scatter plot. (F) Correlation (Pearson) between module eigengenes (ME) and pseudotime, as well as tissue (tissue represented as binary values, 0 and 1, indicating normal and cancerous tissues, respectively). *$P < 0.05$, **$P < 0.01$, ***$P < 0.001$. (For interpretation of the references to colour in this figure legend, the reader is referred to the Web version of this article.)

disease. The yellow module was chiefly enriched in Salmonella infection, tight junction, and motor proteins signaling pathways. Intriguingly, the turquoise module was mainly enriched in ATRNL1+KCN + Fib cells, while the blue module was predominantly found in MMP11+Fib. The green and brown modules were mainly found in SFRP4+Fib, and the red and yellow modules were widely

distributed in all fibroblasts (Fig. 5E). Among these, the turquoise module showed a significant negative correlation with both Pseudotime and tumorigenesis ($P < 0.001$), while all other modules showed a positive correlation with Pseudotime and tumorigenesis ($P < 0.001$). Considering the turquoise module's enrichment in ATRNL1+KCNIP4+Fib and its significant positive correlation with Pseudotime in these fibroblasts, it suggests that the turquoise module regulates the differentiation of these fibroblasts, marking an early event in the differentiation of fibroblasts into cancer-associated fibroblasts. The green and brown modules, although enriched in SFRP4+Fib, showed a negative correlation with Pseudotime in these fibroblasts, indicating that these modules may not participate in the differentiation of SFRP4+Fib, but rather maintain their state. Finally, while the red and yellow modules were widely distributed among all fibroblasts, they showed a significant positive correlation with Pseudotime in all fibroblasts except for GSN + Fib ($P < 0.01$), suggesting these modules may play a crucial regulatory role in fibroblast differentiation (Fig. 5F). We constructed co-expression regulatory networks for the genes in these modules, which were used to demonstrate the regulatory relationships of the core genes in these modules (Fig. S4).

To encapsulate, we constructed a gene co-expression regulatory network of the hub genes from these six modules, reflecting the specific co-expression relationships of these regulatory modules. These findings shed light on the complex regulatory network underlying fibroblast differentiation in the ovarian cancer microenvironment.

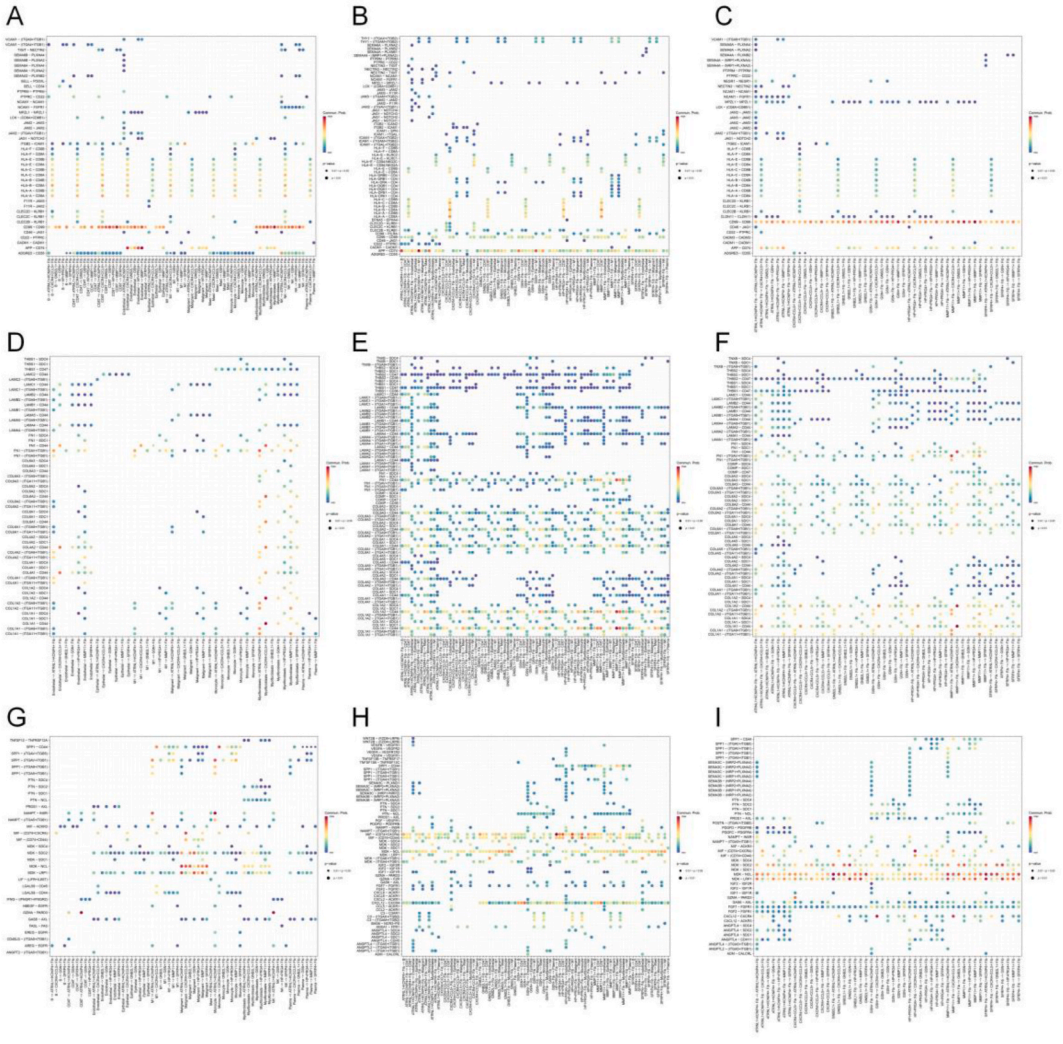

Fig. 6. Cell communication analysis between fibroblasts and multiple cell types in the tumor microenvironment. (A) Cell-Cell Contact analysis of interactions between non-fibroblast cells (sender) and fibroblasts (receiver). (B) Cell-Cell Contact analysis of interactions between fibroblasts (sender) and non-fibroblast cells (receiver). (C) Cell-Cell Contact analysis of interactions between fibroblasts (sender) and other fibroblasts (receiver). (D) ECM-Receptor analysis of interactions between non-fibroblast cells (sender) and fibroblasts (receiver). (E) ECM-Receptor analysis of interactions between fibroblasts (sender) and non-fibroblast cells (receiver). (F) ECM-Receptor analysis of interactions between fibroblasts (sender) and other fibroblasts (receiver). (G) Secreted Signaling analysis of interactions between non-fibroblast cells (sender) and fibroblasts (receiver). (H) Secreted Signaling analysis of interactions between fibroblasts (sender) and non-fibroblast cells (receiver). (I) Secreted Signaling analysis of interactions between fibroblasts (sender) and other fibroblasts (receiver).

The cell-cell communication analysis using CellChat revealed that Endo interacts with Fib in tumor tissues via APP-CD74, while the interaction with ATRNL1+KCNIP4+Fib enriched in normal tissues is not conspicuous. On the other hand, ATRNL1+KCNIP4+Fib interacts with various immune cells such as B, M1, and Monocytes via APP-CD74. Our analysis of Secreted Signaling showed that CD8T

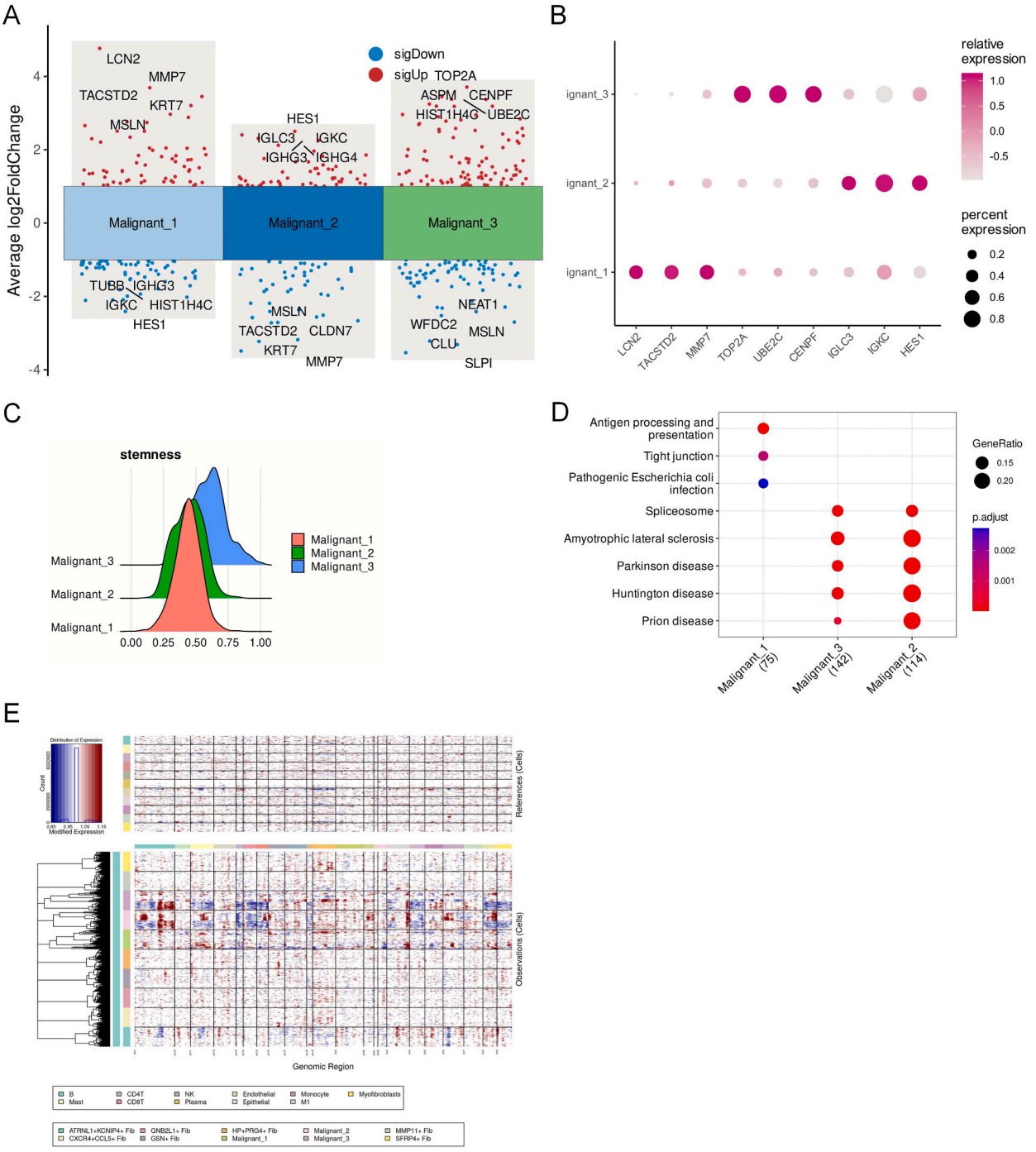

Fig. 7. Analysis of malignant cell subtypes. (A) Differential expression analysis (one vs. others, Wilcoxon test) of malignant cell subtypes (Malignant_1, Malignant_2, Malignant_3). (B) Molecular markers of malignant cell subtypes. (C) Tumor stemness index of malignant cell subtypes. Malignant_3 exhibits the highest tumor stemness. (D) Gene set enrichment analysis of highly expressed genes in malignant cell subtypes. (E) Copy number variation analysis of malignant cells and fibroblasts. It can be observed from the figure that Malignant_1 has a relatively lower degree of copy number variation compared to the other two malignant cell subtypes. Additionally, ATRNL1+KCNIP4+Fib exhibits abnormal copy number variations compared to other normal cells.

and NK cells act on ATRNL1+KCNIP4+Fib via GZMA-PARD3. Malignant cells act on various Fibroblasts via MDK-NCL and MDK-LRP1, and fibroblasts also mainly regulate each other via MDK-NCL, MDK-LRP1 (Fig. 6A, B, C).

Finally, the analysis of ECM-Receptor interaction revealed that MMP11+Fib regulates CD4+T, CD8T, Mast, Monocytes, and CXCR4+CCL5+Fib via ligand-receptor pairs COL1A1-CD44, COL1A2-CD44. These findings provide a comprehensive understanding of fibroblasts' differentiation and interaction within the tumor microenvironment, offering potential therapeutic targets for cancer treatment.

In summary, our investigation focuses on Cancer-associated fibroblasts (CAFs) in ovarian cancer, identifying seven subgroups annotated by their gene markers. Notably, these subgroups exhibit distinct distribution patterns between tumor and normal tissues, with implications for the tumor microenvironment. Differential expression analysis reveals specific pathways enriched in each

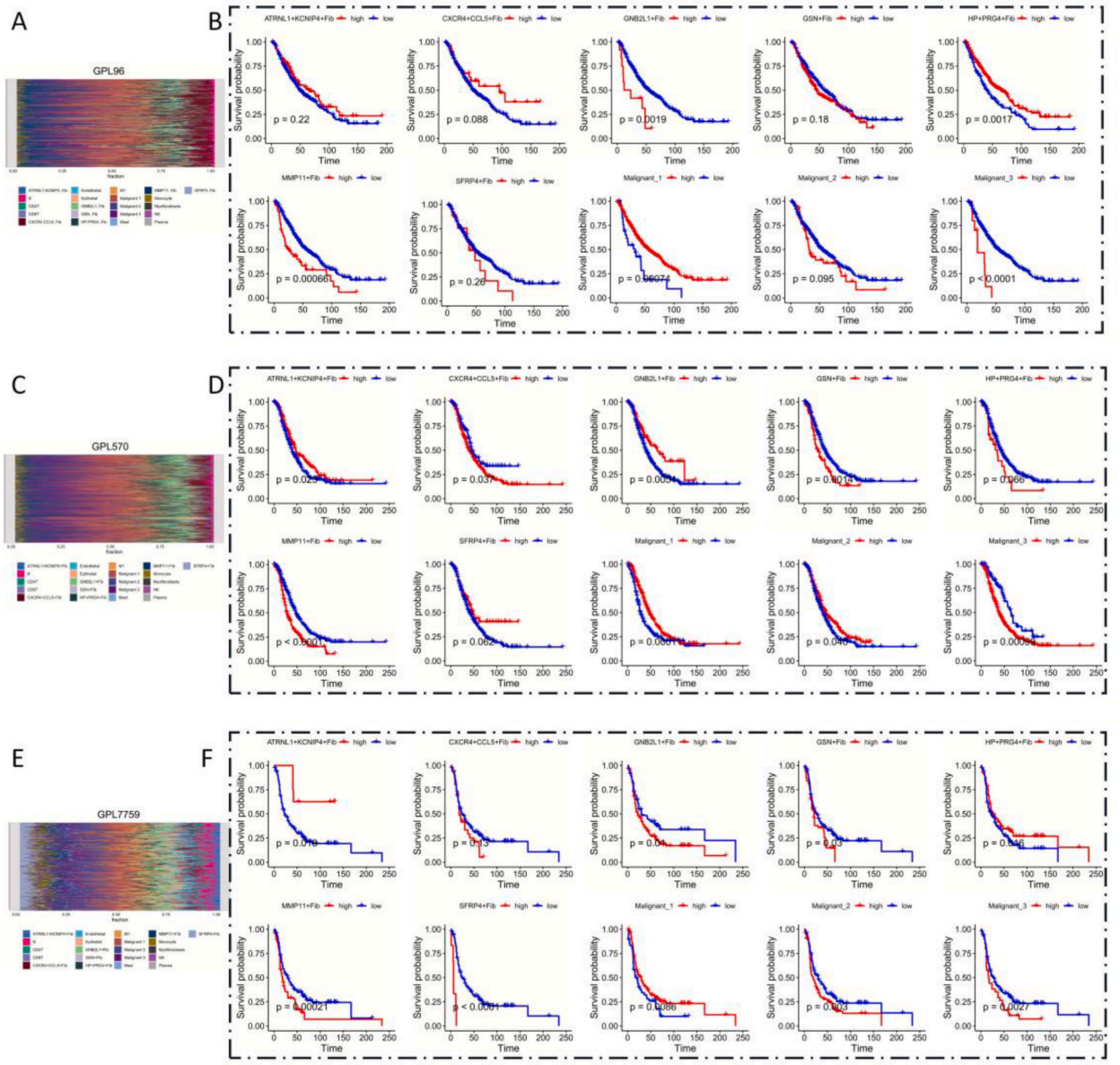

Fig. 8. Relationship between tumor microenvironment and ovarian cancer prognosis. (A) CIBERSORTx scores of tumor microenvironment in the GPL96 cohort. (B) Association between fibroblast subtypes (7 fibroblast subtypes) and malignant cell subtypes (3 malignant cell subtypes) with ovarian cancer prognosis in the GPL96 cohort. (C) CIBERSORTx scores of tumor microenvironment in the GPL570 cohort. (D) Association between fibroblast subtypes (7 fibroblast subtypes) and malignant cell subtypes (3 malignant cell subtypes) with ovarian cancer prognosis in the GPL570 cohort. (E) CIBERSORTx scores of tumor microenvironment in the GPL7759 cohort. (F) Association between fibroblast subtypes (7 fibroblast subtypes) and malignant cell subtypes (3 malignant cell subtypes) with ovarian cancer prognosis in the GPL7759 cohort. The cutoff values for KM curves were determined using the "surv_cutoff" function from the R package "survminer".

fibroblast subtype, shedding light on their functional roles within the tissue. Transcription factor activity analysis highlights key regulatory factors associated with each fibroblast subgroup, providing insights into their activation mechanisms. Additionally, exploration into fibroblast differentiation using CytoTRACE and Monocle2 reveals dynamic trajectories and regulatory modules governing this process. Weighted Gene Co-expression Network Analysis (WGCNA) uncovers co-expression modules associated with fibroblast differentiation and their functional enrichment. Cell-cell communication and secreted signaling analyses elucidate interactions between fibroblasts, immune cells, and malignant cells within the tumor microenvironment. Finally, ECM-Receptor interaction analysis unveils potential therapeutic targets for cancer treatment. Overall, our findings provide a comprehensive understanding of fibroblast differentiation and interactions in ovarian cancer, offering insights into therapeutic strategies targeting the tumor microenvironment.

2.3. Copy number variation analysis of fibroblasts and tumor cells

To further investigate the relationship between fibroblasts and malignant tumor cells, we conducted a study on tumor heterogeneity within the malignant cell cluster (designated as malignant). From this cluster, we identified three subgroups of malignant cells (Malignant_1, Malignant_2, Malignant_3). In Malignant_1, the highly expressed marker genes were LCN2, TACSTD2, and MMP7. Malignant_2 exhibited high expression of the marker genes IGLC3, IGKC, and HES1. In Malignant_3, the highly expressed marker genes included TOP2A, UBE2C, and CENPF (Fig. 7A and B).

Through stemness analysis of tumor cells, we found that Malignant_3 exhibited significantly higher tumor stemness than Malignant_1 and Malignant_2, suggesting that Malignant_3 represents the most aggressive tumor cell subgroup (Fig. 7C).

Functional enrichment analysis revealed that the highly expressed genes in Malignant_1 (75 genes in total) were primarily enriched in pathways such as antigen processing and presentation, tight junction, and pathogenic *Escherichia coli* infection. The highly expressed genes in Malignant_2 (114 genes) and Malignant_3 (142 genes), on the other hand, were mainly enriched in pathways like spliceosome, amyotrophic lateral sclerosis, and prion disease (Fig. 7D).

Lastly, we employed infercnv to analyze the copy number variations (CNVs) among tumor cells and fibroblast subgroups (Fig. 7E). The results indicated that the CNVs in the ATRNL1+KCNIP4+Fib subgroup of fibroblasts were more abnormal compared to other fibroblast types, with low copy number regions on chromosomes 1 and 3, and high copy number regions on chromosomes 2, 4, 16, 17, 18, 21, and 22. Malignant_1 exhibited a completely different pattern of copy number variations compared to Malignant_2 and Malignant_3, with higher copy number variations on chromosome 1 in Malignant_2 and Malignant_3, and lower copy number variations on chromosomes 5, 6, 7, 17, 21, and 22.

These findings suggest that chromosomal copy number abnormalities were already present in the ATRNL1+KCNIP4+Fib in peritumoral tissues. Furthermore, the degree of chromosomal variations was lower in the Malignant_1 subgroup within the malignant cell cluster.

2.4. Ovarian cancer tumor microenvironment analysis

Next, we used CIBERSORTx to deconvolute 3226 samples from the TCGA-OV (374 samples) and other GPL570(738 samples), GSE140082(380 samples), GPL96(438 samples), GPL2986(204 samples), GPL6480(677 samples), GPL7759(415 samples) cohorts. Through deconvolution, we obtained the Absolute scores for 21 cell subgroups (ATRNL1+KCNIP4+Fib, B, CD4T, CD8T, CXCR4+CCL5+Fib, Endothelial, Epithelial, GNB2L1+Fib, GSN + Fib, HP + PRG4+Fib, M1, Malignant 1, Malignant 2, Malignant 3, Mast, MMP11+Fib, Monocyte, Myofibroblasts, NK, Plasma, SFRP4+Fib) in these samples (Fig. 8A–C, E).

In the TCGA-OV cohort, univariate Cox regression analysis revealed that Plasma (beta<0, HR < 1, $P < 0.01$) is a favorable prognostic factor in ovarian cancer, while SFRP4+Fib, GSN + Fib, and MMP11+Fib are unfavorable prognostic factors (beta>0, HR > 1, $P < 0.05$). In the GPL570 cohort, we found that GSN + Fib, MMP11+Fib, and Myofibroblasts are unfavorable prognostic factors for ovarian cancer (beta>0, HR > 1, $P < 0.01$) (CellTypeRisk.xlsx).

Subsequently, we compared the prognosis of ovarian cancer with high and low infiltration of seven fibroblast subgroups using KM curves in six large cohorts (GPL96, GPL570, GPL2986, GPL7759, GPL140082, TCGA OV). The cut-off value was calculated using the surv_cutoff function in the survminer package (Fig. 8B–D, F; Fig. S5). In the GPL96 cohort, high infiltration of GNB2L1+Fib and MMP11+Fib was associated with unfavorable prognosis in ovarian cancer, while a higher infiltration score of HP + PRG4+Fib was a favorable prognostic factor ($P < 0.01$) (Fig. 8A and B). In the GPL570 cohort, patients with ovarian cancer who had higher infiltration of ATRNL1+KCNIP4+Fib and GNB2L1+Fib had better outcomes ($P < 0.05$). High infiltration of CXCR4+CCL5+Fib, GSN + Fib, and MMP11+Fib was an unfavorable prognostic factor in ovarian cancer patients ($P < 0.05$) (Fig. 8C and D). In the GPL2986 cohort, ATRNL1+KCNIP4+Fib, GSN + Fib, HP + PRG4+Fib, and MMP11+Fib high infiltration was an unfavorable prognostic factor in ovarian cancer ($P < 0.05$) (Figs. S5A and B). In the GPL7759 cohort, high infiltration of GNB2L1+Fib, GSN + Fib, MMP11+Fib, and SFRP4+Fib was associated with an unfavorable prognosis in ovarian cancer ($P < 0.05$), while HP + PRG4+Fib and ATRNL1+KCNIP4+Fib were favorable factors ($P < 0.05$) (Fig. 8E and F). In the GPL140082 cohort, high infiltration of CXCR4+CCL5+Fib and HP + PRG4+Fib were favorable prognostic factors in ovarian cancer ($P < 0.05$). High infiltration of GNB2L1+Fib, GSN + Fib, MMP11+Fib, and SFRP4+Fib were unfavorable factors in ovarian cancer ($P < 0.05$) (Fig. S5 C, D). In the TCGA OV cohort, high infiltration of ATRNL1+KCNIP4+Fib was a favorable prognostic factor in ovarian cancer ($P < 0.05$), while GSN + Fib, MMP11+Fib, and SFRP4+Fib were unfavorable prognostic factors (Fig. S5 E, F).

In summary, although the results differ among cohorts, high infiltration of MMP11+Fib, GSN + Fib, and SFRP4+Fib are consistently unfavorable prognostic factors in ovarian cancer. Conversely, ATRNL1+KCNIP4+Fib and HP + PRG4+Fib may convey a

favorable prognosis for ovarian cancer patients. Combining the above analysis, we found that MMP11+Fib represents a high-risk factor for ovarian cancer prognosis.

2.5. SMR analysis identifies EQTLs associated with fibroblast differentiation

Through Summary data-based Mendelian Randomization (SMR) analysis integrating EQTL data from GTex v8 ovary tissue and the ovarian cancer dataset from the GWAS catalog, we identified 2419 genes with EQTLs (Fig. 9A). We charted the distribution of these genes across chromosomes, with the highest number found on chromosome 1 (212 genes, 9%), and the lowest on chromosome 2 (30 genes, 1%) (Fig. 9B). Among these, 132 genes were associated with fibroblast differentiation. These genes are implicated in pathways related to drug metabolism-other enzymes, platinum drug resistance, glutathione metabolism, and one carbon pool by folate. Gene Ontology (GO) analysis revealed associations with mismatch repair and metabolic pathways. These findings underscore a potential critical link between genes related to fibroblast differentiation and drug resistance in ovarian cancer (Fig. 9C and D).

EQTLs (expression quantitative trait loci) are genomic loci that explain a portion of the genetic variance of a gene's expression level. They can provide insights into the mechanisms of complex diseases and traits. In our analysis, we found 132 genes with EQTLs associated with fibroblast differentiation. These genes are involved in pathways related to platinum drug resistance and glutathione metabolism, among others. Platinum-based chemotherapy drugs, such as cisplatin and carboplatin, are standard treatments for ovarian cancer. However, many patients eventually develop resistance to these drugs, which limits their effectiveness. One of the identified pathways, "platinum drug resistance," likely involves mechanisms that protect cancer cells from platinum-induced DNA damage. Our results also indicate that genes involved in the "glutathione metabolism" pathway could be associated with chemoresistance in ovarian cancer. Glutathione is an antioxidant that protects cells from damage. However, in cancer cells, it can confer resistance to chemotherapeutic drugs by neutralizing their effects.

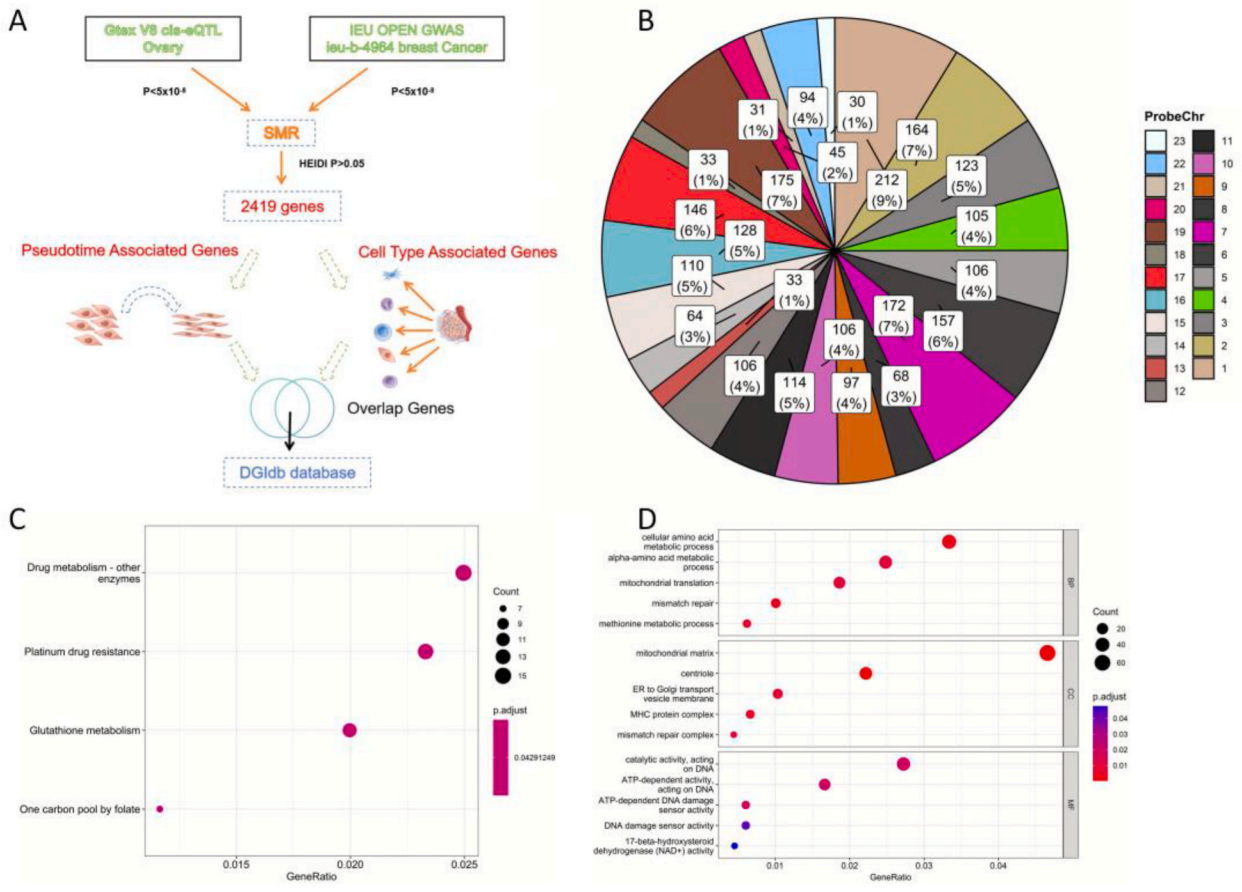

Fig. 9. SMR analysis. (A) Workflow of SMR analysis. (B) Chromosomal distribution of 2419 *cis*-eQTL (GTEx V8 ovary) genes associated with ovarian cancer (ieu-b-4964, breast cancer). (C) KEGG functional enrichment analysis results of 132 *cis*-eQTL genes associated with Pseudotime. (D) GO functional enrichment analysis results of 132 *cis*-eQTL genes associated with Pseudotime.

2.6. Cell-specific eQTLs in the ovarian cancer tumor microenvironment

Next, we performed an eQTL analysis on the highly expressed genes of 21 types of cell populations present within the tumor microenvironment **(Data Supplement.xlsx)**.

In the malignant cell population 1 (Malignant1), we identified seven genes associated with ovarian cancer exhibiting eQTL effects. Using the DGIdb database (http://www.dgidb.org), PAX8, PPA1, and NDUFC2 were found to have 69 drug-gene interaction hits (see Supplementary Information). In the malignant cell population 2 (Malignant2), we detected 14 genes associated with ovarian cancer demonstrating eQTL effects. Similarly, PPA1, NME1, and MIF were discovered to have 6 drug-gene interaction hits. In the malignant cell population 3 (Malignant3), we revealed three genes associated with ovarian cancer with eQTL effects. Among these genes, only DHFR had 15 drug-gene interaction hits.

Furthermore, in the analysis of fibroblast subtypes, a total of 66 genes with eQTL effects were found in the ATRNL1+KCNIP4+Fib subtype. Among these genes, GSTM3, ACYP2, ANXA5, ASPH, HEBP1, MARK3, ENOSF1, APOE, ERCC1 had a total of 67 drug-gene interaction hits.

Notably, the MMP11+Fib subtype had five genes associated with ovarian cancer showing eQTL effects (FAM114A1, CPE, PPIC, TMED9, RAB31). Although no drugs associated with these genes were found in the DGIdb database, drugs targeting these genes could serve as potential avenues for future development.

We have included the genes from other cell types exhibiting eQTL effects associated with ovarian cancer in the Supplementary Information. Further research into these findings could provide new insights into the cellular dynamics of the ovarian cancer tumor microenvironment and lead to the development of new therapeutic strategies.

3. Discussion

Ovarian cancer-associated fibroblasts (CAFs) have been identified as pivotal contributors to tumor cell proliferation, invasion, and metastasis [51]. Cancer-associated fibroblasts play an important role in the tumour microenvironment, while studies related to their differentiation patterns and their subpopulation composition remain scarce.

Our significant contributions to this research have been the deep analysis of the tumor microenvironment in ovarian cancer. We identified 13 primary cell populations within ovarian cancer tissue, including CD8T, Malignant, Fibroblasts, CD4T, NK, M1, Monocyte, Epithelial, Myofibroblast, Endothelial, Plasma, B, and Mast cells. By contrasting the tissue microenvironments of ovarian cancer and normal ovarian tissue, we observed marked discrepancies. Normal tissue displayed a higher proportion of stromal cells, with fibroblasts being predominant. Fibroblast cells play a key physiological role in normal tissue, synthesizing and secreting collagen, elastin, and other matrix molecules to maintain tissue structural integrity and participate in growth, repair, and regeneration processes. The higher infiltration of CD8+T and CD4+T cells in tumor tissue aligns with previous studies and is generally considered a crucial indicator of tumor immune response, as these cells are the main executors of the tumor immune response, promoting tumor cell clearance and immune surveillance [52,53].

Our comprehensive study scrutinised the transcription factor (TF) activity of 13 cellular populations within ovarian cancer tissue and normal ovarian tissue. Our findings shine light on the underexplored role of the activated transcription factor FOXA2 in cancer-associated mast cells, with its activity significantly higher in tumor tissue compared to normal tissue. Despite FOXA2 being known for its crucial role in Th2 immune response activation [54], the biological implications of its heightened activity in mast cells within tumor tissue warrant further investigation.

Intriguingly, we also observed a significant increase in the activity of FOXA1 in several cell types within tumor tissues. Endothelial cells, myofibroblasts, epithelial cells, and fibroblasts all exhibited heightened FOXA1 activity compared to their counterparts in normal tissue. This transcription factor was also notably activated in malignant cells. Previous studies have established FOXA1 as a serum biomarker for ovarian cancer, with overexpression evident in ovarian tumor tissue [55]. Its role in influencing the progression and prognosis of breast and prostate cancer has also been documented, suggesting a notable influence on cancer biology [56,57].

Continuing, our analysis of signalling pathway activity across the 13 cell types revealed distinct patterns. For instance, the TGF-beta pathway in fibroblasts was significantly more active in tumor tissue compared to normal tissue, while no discernible difference was observed in myofibroblasts. This aligns with previous findings that cancer-associated fibroblasts drive CXCL13 production in activated T cells via TGF-beta [58]. Key molecules regulating CAFs in hypoxia include TGF-beta and hypoxia-inducible factors (HIFs), which modulate several mechanisms inducing cancer malignancy, such as extracellular matrix (ECM) remodelling, immune evasion, metabolic reprogramming, angiogenesis, metastasis, and drug resistance [59].

Lastly, the p53 pathway in epithelial cells was markedly more active in tumor tissue than in normal tissue. The TP53 signaling pathway plays a vital role in cellular stress response, stimulating cell cycle arrest, DNA repair, and apoptosis in response to various stresses and damages to maintain cellular homeostasis and overall genomic stability [60]. Many tumor cells harbor TP53 mutations or functional defects, resulting in a reduced response to DNA damage and other stress factors, thereby increasing the survival and proliferation ability of tumor cells [61]. This ultimately contributes to malignancy and cancer development. Thus, alterations in the TP53 signaling pathway are often intimately linked with the onset, progression, and treatment resistance of tumors [62]. Our study uncovers distinctive transcriptional and pathway dynamics within ovarian cancer, underlining the potential significance of FOXA1 and FOXA2 in different cell types, and highlighting the role of key signaling pathways, such as TGF-beta and TP53. These findings provide a solid foundation for future investigations into the complex molecular mechanisms underlying ovarian cancer progression.

Given the pivotal role of cancer-associated fibroblasts (CAFs) in the microenvironment of ovarian cancer, we embarked on a detailed investigation of the heterogeneity of fibroblasts in ovarian cancer tissues. We identified seven subgroups of fibroblasts:

ATRNL1+KCN + Fib (cluster0), MMP11+Fib (cluster1), SFRP4+Fib (cluster2), GNB2L1+Fib (cluster3), HP + PRG4+Fib (cluster4), GSN + Fib (cluster5), and CXCR4+CCL5+Fib(cluster6). Each fibroblast subgroup exhibits unique transcription factors and activated signaling pathways. Single-cell pseudo-time analysis revealed that ATRNL1+KCN + Fib, predominantly present in peritumoral tissues, represents the earliest differentiation stage of fibroblasts. Gene Set Enrichment Analysis (GSEA) of genes driving fibroblast differentiation identified Proteasome, Spliceosome, and Oxidative Phosphorylation as the principal signaling pathways. Oxidative Phosphorylation is a significant feature of metabolic reprogramming, as supported by studies showing that TRAP1 suppresses the progression of oral squamous cell carcinoma by reducing oxidative phosphorylation metabolism of cancer-associated fibroblasts [63].

Moreover, we discovered that fibroblasts can terminally differentiate from the initial state of ATRNL1+KCN + Fib into two states: SFRP4+Fib and MMP11+Fib. This indicates that the formation of cancer-associated fibroblasts (CAFs) is not a singular pathway but differentiates into various CAF types depending on the tumor microenvironment state. CAFs differentiating towards MMP11+Fib are primarily regulated by Cytokine-cytokine receptor interaction, Legionellosis, and NF-kappa B signaling pathway. MMP11 plays a crucial role in tumor development and progression [25,64]. Matrix metalloproteinases (MMPs), a family of zinc-dependent endopeptidases, degrade almost all ECM proteins to remodel the extracellular matrix (ECM), playing a vital role in the invasion and metastasis of solid malignancies [65]. High expression of MMP11 in fibroblasts is associated with cancer cell proliferation and coincides with activation of the TGFβ signaling pathway [66].

To further explore the role of fibroblasts in the tumor microenvironment, we used CellChat to analyze cellular communication between fibroblasts and other cells in the tumor microenvironment. We found that MMP11+Fib regulated CD4+T, CD8T, Mast, Monocyte via the receptor-ligand pairs COL1A1-CD44, COL1A2-CD44. CD44 plays vital roles in cell-cell and cell-matrix interactions, particularly under pathophysiologic conditions. In vitro studies have shown that CD44 is critical for MMP-dependent transforming growth factor-beta (TGF-β) activation and directional fibroblast migration [67].

Next, we investigated the relationship between the ovarian cancer tumor microenvironment and prognosis using a large sample size across six platforms. Using Kaplan-Meier curves to compare the infiltration levels of the seven fibroblast subgroups with the prognosis of ovarian cancer in six large cohorts (GPL96, GPL570, GPL2986, GPL7759, GPL140082, TCGA OV), we found that high infiltration of MMP11+Fib, GSN + Fib, SFRP4+Fib was a negative prognostic factor for ovarian cancer. ATRNL1+KCNIP4+Fib and HP + PRG4+Fib might be beneficial for the prognosis of ovarian cancer patients.

In summary, this study provides valuable insights into the crucial role and complexity of fibroblasts in ovarian cancer. Through single-cell analysis, we have unveiled the diversity of fibroblasts in ovarian cancer tissues, identified multiple subgroups, and delved into their function and regulatory mechanisms. This research offers new potential for drug development and therapeutic strategy design by applying Mendelian randomization to explore the causal relationship of the tumor microenvironment and analyzing genes with potential drug targets. Our findings provide beneficial guidance for future clinical practice and research. Nonetheless, many questions remain to be explored, such as the interaction between different fibroblast subgroups, validation of potential drug targets, which will be one of the future research directions. However, the results of these studies are built on large-scale histological sequencing technology and require more biological experiments to prove them.

Consent for publication

The Authors confirm.

- That the work described has not been published before (except in the form of an abstract or as part of a published lecture, review, or thesis);
- That it is not under consideration for publication elsewhere;
- That its publication has been approved by all co-authors, if any;
- That its publication has been approved (tacitly or explicitly) by the responsible authorities at the institution where the work is carried out.

Competing interests

The authors declare that there is no conflict of interest that could be perceived as prejudicial to the impartiality of the reported research.

Funding

This research was funded by the Scientific Research Project of Jiangsu Health Commission (ZDA2020012), Primary Research & Development Plan of Jiangsu Province (SBE2020741118), Jiangsu Provincial Commission of Health (M2022016).

Availability of data and material

All bioinformatics data and analysis codes were sourced from publicly available data queues and data packages. The original experimental data can be obtained by applying to the corresponding author.

CRediT authorship contribution statement

Bo Ding: Visualization, Validation, Methodology, Investigation, Conceptualization. **Zheng Ye:** Methodology, Investigation, Formal analysis, Conceptualization. **Han Yin:** Writing – original draft, Supervision, Investigation, Data curation. **Xin-Yi Hong:** Visualization, Validation, Resources, Formal analysis. **Song-wei Feng:** Writing – review & editing, Writing – original draft, Visualization, Validation, Software. **Jing-Yun Xu:** Supervision, Project administration. **Yang Shen:** Funding acquisition, Data curation, Conceptualization.

Declaration of competing interest

We hereby declare that there are no conflicts of interest that could be perceived as prejudicial to the impartiality of the reported research.

We solemnly declare that neither we nor any of the authors, co-authors, or participants involved in this research have any direct or indirect financial, personal, or professional relationships with individuals, organizations, or entities that could create conflicts of interest in relation to the subject matter of this study.

Conflicts of interest, in this context, include but are not limited to financial relationships with companies or organizations relevant to the research field, employment or consulting arrangements, ownership of shares in relevant companies, or any other personal or professional connections that could be perceived as biasing or potentially biasing.

We affirm that the design, implementation, data analysis, and interpretation of this study strictly adhered to principles of scientific ethics and professional conduct.

We make this declaration to ensure transparency in our research and to enable readers to assess any potential impact of conflicts of interest on the study or its findings.

We believe that this declaration provides sufficient information for readers to independently judge the reliability and credibility of the research.

Should there be any further questions or need for additional information, please feel free to contact us.

Acknowledgements

Thanks to the TCGA (The Cancer Genome Atlas) and GEO (Gene Expression Omnibus) working group for providing public data for this study.

Appendix A. Supplementary data

Supplementary data to this article can be found online at https://doi.org/10.1016/j.heliyon.2024.e27873.

References

[1] T. Arora, S. Mullangi, M.R. Lekkala, Ovarian Cancer, 2021.
[2] M. Zhang, Z. Chen, Y. Wang, H. Zhao, Y. Du, The role of cancer-associated fibroblasts in ovarian cancer, Cancers 14 (2022) 2637.
[3] F. Bray, J. Ferlay, I. Soerjomataram, R.L. Siegel, L.A. Torre, A. Jemal, Global cancer statistics 2018: GLOBOCAN estimates of incidence and mortality worldwide for 36 cancers in 185 countries, CA A Cancer J. Clin. 68 (2018) 394–424.
[4] D.-J. Cheon, Y. Tong, M.-S. Sim, J. Dering, D. Berel, X. Cui, J. Lester, J.A. Beach, M. Tighiouart, A.E. Walts, A collagen-remodeling gene signature regulated by TGF-β signaling is associated with metastasis and poor survival in serous ovarian cancer, Clin. Cancer Res. 20 (2014) 711–723.
[5] N. Colombo, C. Sessa, A. du Bois, J. Ledermann, W.G. McCluggage, I. McNeish, P. Morice, S. Pignata, I. Ray-Coquard, I. Vergote, ESMO–ESGO consensus conference recommendations on ovarian cancer: pathology and molecular biology, early and advanced stages, borderline tumours and recurrent disease, Ann. Oncol. 30 (2019) 672–705.
[6] S.-J. Chang, R.E. Bristow, D.S. Chi, W.A. Cliby, Role of aggressive surgical cytoreduction in advanced ovarian cancer, Journal of gynecologic oncology 26 (2015) 336–342.
[7] N. Singh, D. Badrun, P. Ghatage, State of the art and up-and-coming angiogenesis inhibitors for ovarian cancer, Expet Opin. Pharmacother. 21 (2020) 1579–1590.
[8] K. Odunsi, Immunotherapy in ovarian cancer, Ann. Oncol. 28 (2017) viii1–viii7.
[9] Y. Yang, Y. Yang, J. Yang, X. Zhao, X. Wei, Tumor microenvironment in ovarian cancer: function and therapeutic strategy, Front. Cell Dev. Biol. 8 (2020) 758.
[10] Y. Yuan, Y.-C. Jiang, C.-K. Sun, Q.-M. Chen, Role of the tumor microenvironment in tumor progression and the clinical applications, Oncol. Rep. 35 (2016) 2499–2515.
[11] O. Maller, H. Martinson, P. Schedin, Extracellular matrix composition reveals complex and dynamic stromal-epithelial interactions in the mammary gland, J. Mammary Gland Biol. Neoplasia 15 (2010) 301–318.
[12] M. Desbois, Y. Wang, Cancer-associated fibroblasts: key players in shaping the tumor immune microenvironment, Immunol. Rev. 302 (2021) 241–258.
[13] S. Dasari, Y. Fang, A.K. Mitra, Cancer associated fibroblasts: naughty neighbors that drive ovarian cancer progression, Cancers 10 (2018) 406.
[14] X. Xiang, Y.-R. Niu, Z.-H. Wang, L.-L. Ye, W.-B. Peng, Q. Zhou, Cancer-associated Fibroblasts: Vital Suppressors of the Immune Response in the Tumor Microenvironment, Cytokine & Growth Factor Reviews, 2022.
[15] M. Hilmi, R. Nicolle, C. Bousquet, C. Neuzillet, Cancer-associated fibroblasts: accomplices in the tumor immune evasion, Cancers 12 (2020) 2969.
[16] Y. Ni, X. Zhou, J. Yang, H. Shi, H. Li, X. Zhao, X. Ma, The role of tumor-stroma interactions in drug resistance within tumor microenvironment, Front. Cell Dev. Biol. 9 (2021) 637675.
[17] T. Liu, C. Han, S. Wang, P. Fang, Z. Ma, L. Xu, R. Yin, Cancer-associated fibroblasts: an emerging target of anti-cancer immunotherapy, J. Hematol. Oncol. 12 (2019) 1–15.

[18] M. Nurmik, P. Ullmann, F. Rodriguez, S. Haan, E. Letellier, In search of definitions: cancer-associated fibroblasts and their markers, Int. J. Cancer 146 (2020) 895–905.
[19] H. Jiang, S. Hegde, B.L. Knolhoff, Y. Zhu, J.M. Herndon, M.A. Meyer, T.M. Nywening, W.G. Hawkins, I.M. Shapiro, D.T. Weaver, Targeting focal adhesion kinase renders pancreatic cancers responsive to checkpoint immunotherapy, Nat. Med. 22 (2016) 851–860.
[20] K.P. Olive, M.A. Jacobetz, C.J. Davidson, A. Gopinathan, D. McIntyre, D. Honess, B. Madhu, M.A. Goldgraben, M.E. Caldwell, D. Allard, Inhibition of Hedgehog signaling enhances delivery of chemotherapy in a mouse model of pancreatic cancer, Science 324 (2009) 1457–1461.
[21] K. Pietras, J. Pahler, G. Bergers, D. Hanahan, Functions of paracrine PDGF signaling in the proangiogenic tumor stroma revealed by pharmacological targeting, PLoS Med. 5 (2008) e19.
[22] J. Qian, S. Olbrecht, B. Boeckx, H. Vos, D. Laoui, E. Etlioglu, E. Wauters, V. Pomella, S. Verbandt, P. Busschaert, A pan-cancer blueprint of the heterogeneous tumor microenvironment revealed by single-cell profiling, Cell Res. 30 (2020) 745–762.
[23] H.Q. Dinh, X. Lin, F. Abbasi, R. Nameki, M. Haro, C.E. Olingy, H. Chang, L. Hernandez, S.A. Gayther, K.N. Wright, Single-cell transcriptomics identifies gene expression networks driving differentiation and tumorigenesis in the human fallopian tube, Cell Rep. 35 (2021).
[24] L. Geistlinger, S. Oh, M. Ramos, L. Schiffer, R.S. LaRue, C.M. Henzler, S.A. Munro, C. Daughters, A.C. Nelson, B.J. Winterhoff, Multiomic analysis of subtype evolution and heterogeneity in high-grade serous ovarian carcinoma, Cancer Res. 80 (2020) 4335–4345.
[25] J. Xu, Y. Fang, K. Chen, S. Li, S. Tang, Y. Ren, Y. Cen, W. Fei, B. Zhang, Y. Shen, Single-cell RNA sequencing reveals the tissue architecture in human high-grade serous ovarian cancer, Clin. Cancer Res. 28 (2022) 3590–3602.
[26] J. Liu, T. Lichtenberg, K.A. Hoadley, L.M. Poisson, A.J. Lazar, A.D. Cherniack, A.J. Kovatich, C.C. Benz, D.A. Levine, A.V. Lee, An integrated TCGA pan-cancer clinical data resource to drive high-quality survival outcome analytics, Cell 173 (2018) 400–416. e411.
[27] J.T. Leek, W.E. Johnson, H.S. Parker, A.E. Jaffe, J.D. Storey, The sva package for removing batch effects and other unwanted variation in high-throughput experiments, Bioinformatics 28 (2012) 882–883.
[28] B. Elsworth, M. Lyon, T. Alexander, Y. Liu, P. Matthews, J. Hallett, P. Bates, T. Palmer, V. Haberland, G.D. Smith, The MRC IEU OpenGWAS data infrastructure, bioRxiv (2020), 2020.08.10.244293.
[29] G. Consortium, The GTEx Consortium atlas of genetic regulatory effects across human tissues, Science 369 (2020) 1318–1330.
[30] C. Hafemeister, R. Satija, Normalization and variance stabilization of single-cell RNA-seq data using regularized negative binomial regression, Genome Biol. 20 (2019) 296.
[31] I. Korsunsky, N. Millard, J. Fan, K. Slowikowski, F. Zhang, K. Wei, Y. Baglaenko, M. Brenner, P.-r. Loh, S. Raychaudhuri, Fast, sensitive and accurate integration of single-cell data with Harmony, Nat. Methods 16 (2019) 1289–1296.
[32] D. Aran, A.P. Looney, L. Liu, E. Wu, V. Fong, A. Hsu, S. Chak, R.P. Naikawadi, P.J. Wolters, A.R. Abate, Reference-based analysis of lung single-cell sequencing reveals a transitional profibrotic macrophage, Nat. Immunol. 20 (2019) 163–172.
[33] Y. Han, Y. Wang, X. Dong, D. Sun, Z. Liu, J. Yue, H. Wang, T. Li, C. Wang, TISCH2: expanded datasets and new tools for single-cell transcriptome analyses of the tumor microenvironment, Nucleic Acids Res. 51 (2023) D1425–D1431.
[34] G.S. Gulati, S.S. Sikandar, D.J. Wesche, A. Manjunath, A. Bharadwaj, M.J. Berger, F. Ilagan, A.H. Kuo, R.W. Hsieh, S. Cai, Single-cell transcriptional diversity is a hallmark of developmental potential, Science 367 (2020) 405–411.
[35] X. Qiu, Q. Mao, Y. Tang, L. Wang, R. Chawla, H.A. Pliner, C. Trapnell, Reversed graph embedding resolves complex single-cell trajectories, Nat. Methods 14 (2017) 979–982.
[36] P. Langfelder, S. Horvath, WGCNA: an R package for weighted correlation network analysis, BMC Bioinf. 9 (2008) 1–13.
[37] S. Morabito, F. Reese, N. Rahimzadeh, E. Miyoshi, V. Swarup, hdWGCNA identifies co-expression networks in high-dimensional transcriptomics data, Cell Reports Methods (2023).
[38] M.A. Durante, D.A. Rodriguez, S. Kurtenbach, J.N. Kuznetsov, M.I. Sanchez, C.L. Decatur, H. Snyder, L.G. Feun, A.S. Livingstone, J.W. Harbour, Single-cell analysis reveals new evolutionary complexity in uveal melanoma, Nat. Commun. 11 (2020) 496.
[39] C.H. Holland, J. Tanevski, J. Perales-Patón, J. Gleixner, M.P. Kumar, E. Mereu, B.A. Joughin, O. Stegle, D.A. Lauffenburger, H. Heyn, Robustness and applicability of transcription factor and pathway analysis tools on single-cell RNA-seq data, Genome Biol. 21 (2020) 1–19.
[40] N. Rusk, Expanded CIBERSORTx, Nat. Methods 16 (2019) 577, 577.
[41] S. Jin, C.F. Guerrero-Juarez, L. Zhang, I. Chang, R. Ramos, C.H. Kuan, P. Myung, M.V. Plikus, Q. Nie, Inference and analysis of cell-cell communication using CellChat, Nat. Commun. 12 (2021) 1088.
[42] Z. Zhu, F. Zhang, H. Hu, A. Bakshi, M.R. Robinson, J.E. Powell, G.W. Montgomery, M.E. Goddard, N.R. Wray, P.M. Visscher, Integration of summary data from GWAS and eQTL studies predicts complex trait gene targets, Nat. Genet. 48 (2016) 481–487.
[43] Y. Wu, J. Zeng, F. Zhang, Z. Zhu, T. Qi, Z. Zheng, L.R. Lloyd-Jones, R.E. Marioni, N.G. Martin, G.W. Montgomery, Integrative analysis of omics summary data reveals putative mechanisms underlying complex traits, Nat. Commun. 9 (2018) 918.
[44] D.G. Bunis, J. Andrews, G.K. Fragiadakis, T.D. Burt, M. Sirota, dittoSeq: universal user-friendly single-cell and bulk RNA sequencing visualization toolkit, Bioinformatics 36 (2020) 5535–5536.
[45] L. Zeng, X. Wang, F. Wang, X. Zhao, Y. Ding, Identification of a gene signature of cancer-associated fibroblasts to predict prognosis in ovarian cancer, Front. Genet. 13 (2022) 925231.
[46] J. Bai, Z. Jiang, X. Zhao, N. Wang, A. Chen, Y. Luo, Cancer-associated fibroblast-related genes are associated with prognosis of patients with ovarian cancer, Russ. J. Genet. 59 (2023) S208–S218.
[47] J. Paulsson, P. Micke, Prognostic Relevance of Cancer-Associated Fibroblasts in Human Cancer, Seminars in Cancer Biology, Elsevier, 2014, pp. 61–68.
[48] P. Badia-i-Mompel, J. Vélez Santiago, J. Braunger, C. Geiss, D. Dimitrov, S. Müller-Dott, P. Taus, A. Dugourd, C.H. Holland, R.O. Ramirez Flores, decoupleR: ensemble of computational methods to infer biological activities from omics data, Bioinformatics Advances 2 (2022) vbac016.
[49] M. Pickup, S. Novitskiy, H.L. Moses, The roles of TGFβ in the tumour microenvironment, Nat. Rev. Cancer 13 (2013) 788–799.
[50] S. Hänzelmann, R. Castelo, J. Guinney, GSVA: gene set variation analysis for microarray and RNA-seq data, BMC Bioinf. 14 (2013) 1–15.
[51] Y. Zhang, H. Tang, J. Cai, T. Zhang, J. Guo, D. Feng, Z. Wang, Ovarian cancer-associated fibroblasts contribute to epithelial ovarian carcinoma metastasis by promoting angiogenesis, lymphangiogenesis and tumor cell invasion, Cancer Lett. 303 (2011) 47–55.
[52] M. Oshi, M. Asaoka, Y. Tokumaru, L. Yan, R. Matsuyama, T. Ishikawa, I. Endo, K. Takabe, CD8 T cell score as a prognostic biomarker for triple negative breast cancer, Int. J. Mol. Sci. 21 (2020) 6968.
[53] A.M. Miggelbrink, J.D. Jackson, S.J. Lorrey, E.S. Srinivasan, J. Waibl-Polania, D.S. Wilkinson, P.E. Fecci, CD4 T-cell exhaustion: does it exist and what are its roles in cancer? Clin. Cancer Res. 27 (2021) 5742–5752.
[54] G. Chen, H. Wan, F. Luo, L. Zhang, Y. Xu, I. Lewkowich, M. Wills-Karp, J.A. Whitsett, Foxa2 programs Th2 cell-mediated innate immunity in the developing lung, J. Immunol. 184 (2010) 6133–6141.
[55] Y. Duan, C. Cui, C. Qiu, G. Sun, X. Wang, P. Wang, H. Ye, L. Dai, J. Shi, Serum autoantibodies against LRDD, STC1, and FOXA1 as biomarkers in the detection of ovarian cancer, Dis. Markers (2022) 2022.
[56] A.R. Michmerhuizen, D.E. Spratt, L.J. Pierce, C.W. Speers, ARe we there yet? Understanding androgen receptor signaling in breast cancer, NPJ Breast Cancer 6 (2020) 47.
[57] B. Gui, F. Gui, T. Takai, C. Feng, X. Bai, L. Fazli, X. Dong, S. Liu, X. Zhang, W. Zhang, Selective Targeting of PARP-2 Inhibits Androgen Receptor Signaling and Prostate Cancer Growth through Disruption of FOXA1 Function, vol. 116, Proceedings of the National Academy of Sciences, 2019, pp. 14573–14582.
[58] R.A. O'Connor, B.R. Martinez, L. Koppensteiner, L. Mathieson, A.R. Akram, Cancer-associated fibroblasts drive CXCL13 production in activated T cells via TGF-beta, Front. Immunol. 14 (2023).
[59] I. Kim, S. Choi, S. Yoo, M. Lee, I.-S. Kim, Cancer-associated fibroblasts in the hypoxic tumor microenvironment, Cancers 14 (2022) 3321.
[60] A.H. Stegh, Targeting the p53 signaling pathway in cancer therapy–the promises, challenges and perils, Expert Opin. Ther. Targets 16 (2012) 67–83.

[61] X. Chen, L.J. Ko, L. Jayaraman, C. Prives, p53 levels, functional domains, and DNA damage determine the extent of the apoptotic response of tumor cells, Gene Dev. 10 (1996) 2438–2451.
[62] Z. Liu, H. Guo, Y. Zhu, Y. Xia, J. Cui, K. Shi, Y. Fan, B. Shi, S. Chen, TP53 alterations of hormone-naïve prostate cancer in the Chinese population, Prostate Cancer Prostatic Dis. 24 (2021) 482–491.
[63] L. Xiao, Q. Hu, Y. Peng, K. Zheng, T. Zhang, L. Yang, Z. Wang, W. Tang, J. Yu, Q. Xiao, TRAP1 suppresses oral squamous cell carcinoma progression by reducing oxidative phosphorylation metabolism of Cancer-associated fibroblasts, BMC Cancer 21 (2021) 1329.
[64] X. Zhang, S. Huang, J. Guo, L. Zhou, L. You, T. Zhang, Y. Zhao, Insights into the distinct roles of MMP-11 in tumor biology and future therapeutics, Int. J. Oncol. 48 (2016) 1783–1793.
[65] S. Curran, G.I. Murray, Matrix metalloproteinases in tumour invasion and metastasis, J. Pathol. 189 (1999) 300–308.
[66] N. Eiro, L. González, A. Martínez-Ordoñez, B. Fernandez-Garcia, L.O. González, S. Cid, F. Dominguez, R. Perez-Fernandez, F.J. Vizoso, Cancer-associated fibroblasts affect breast cancer cell gene expression, invasion and angiogenesis, Cell. Oncol. 41 (2018) 369–378.
[67] P. Govindaraju, L. Todd, S. Shetye, J. Monslow, E. Puré, CD44-dependent inflammation, fibrogenesis, and collagenolysis regulates extracellular matrix remodeling and tensile strength during cutaneous wound healing, Matrix Biol. 75 (2019) 314–330.